

U.S. DEPARTMENT OF
ENERGY

Office of
Science

Di-hadron correlations with event shape engineering in Au+Au collisions at the STAR experiment



*Ryo Aoyama, for the **STAR** Collaboration
University of Tsukuba, TCHoU*

Nov. 17th, 2018

Quark and Nuclear Physics @Tsukuba



筑波大学
University of Tsukuba



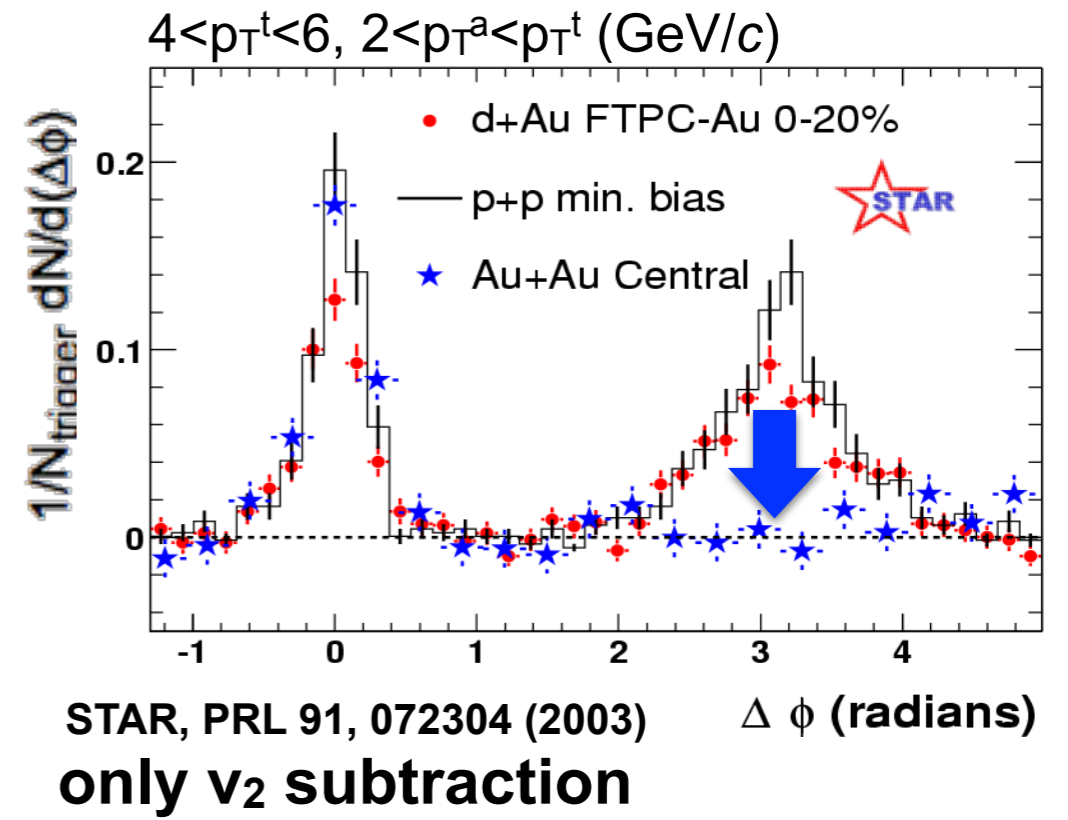
Tomonaga Center
for the History of the Universe



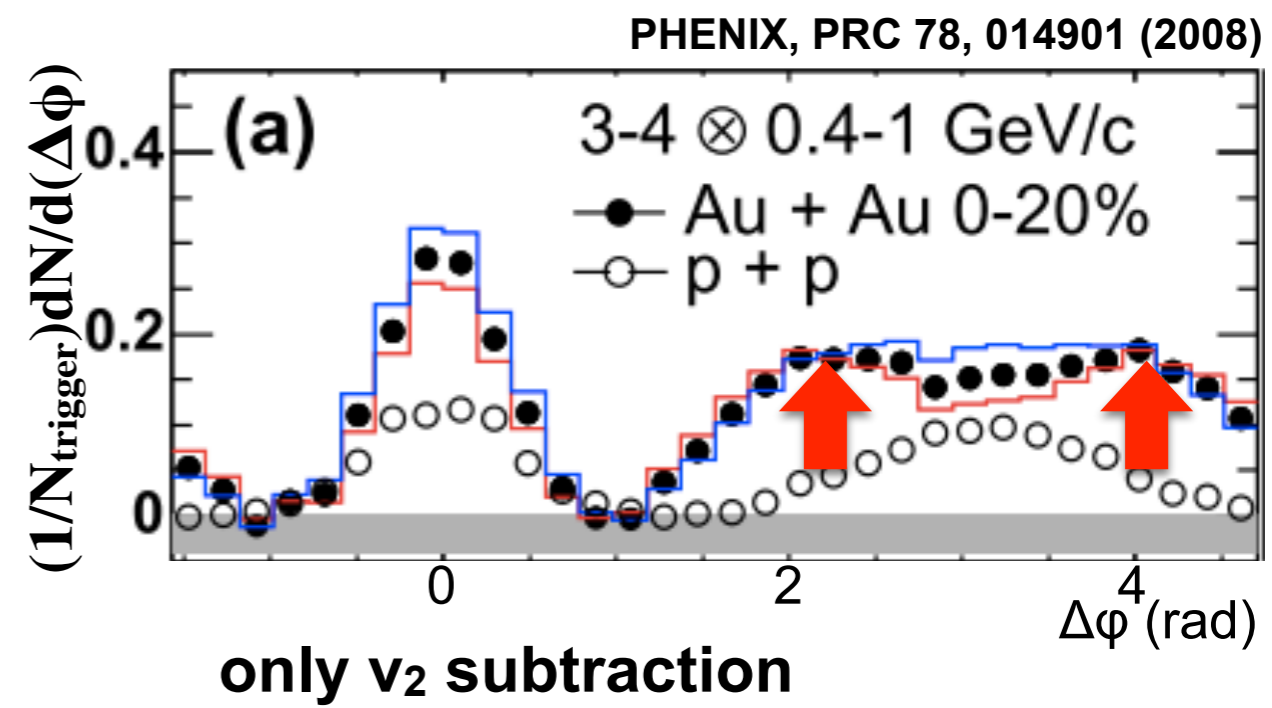
Jets with di-hadron correlations in heavy-ion collisions

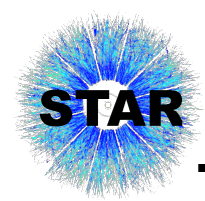
- ◆ Jets interact with colored matter and lose their energy : **jet quenching**
 - ▶ **probe energy loss mechanisms in the QGP**

- ◆ **high- p_T** : disappearance of back-to-back jet-like peak in central Au+Au collisions
 - ▶ **jet suppression in the QGP**



- ◆ **low- p_T** : enhanced yield on both near and away side compared to p+p collisions
 - ▶ **re-distribution of deposited energy**



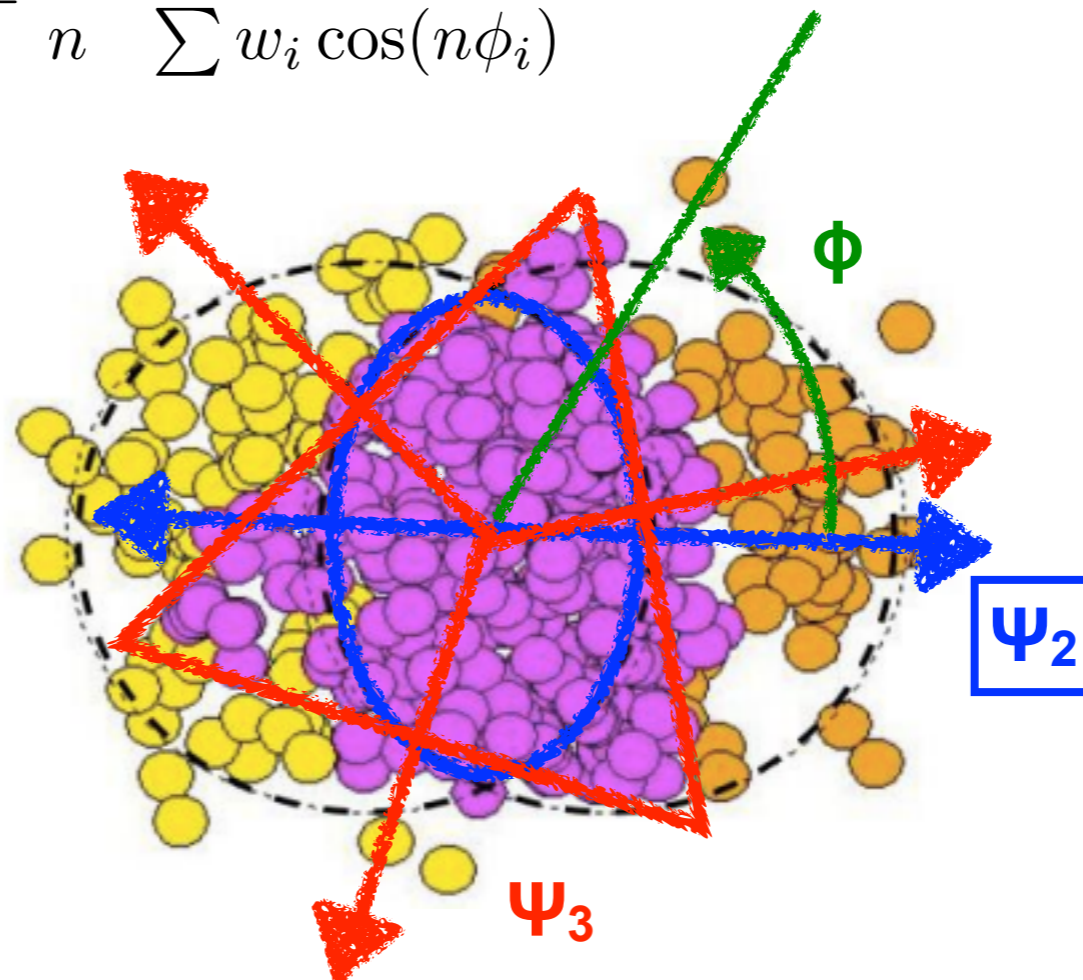


Event plane and higher order flow harmonics

- ◆ Spatial anisotropy due to **almond-like shape** and **event-by-event fluctuations** of overlapping region of nuclei in non-central heavy-ion collisions
- ◆ Deformation converted into momentum space by **collective motion (flow)**
 - azimuthal anisotropy

azimuthal distribution : $\frac{dN}{d\phi} \propto 1 + \sum_i 2v_n \cos n(\phi - \Psi_n)$

n-th order event plane : $\Psi_n = \frac{1}{n} \cdot \frac{\sum w_i \sin(n\phi_i)}{\sum w_i \cos(n\phi_i)}$





Event plane dependent di-hadron correlations

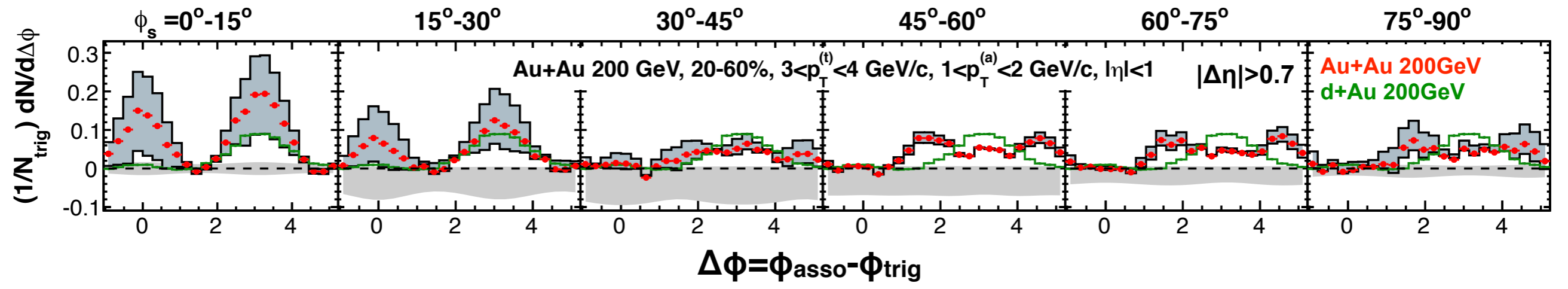
STAR, PRC 89, 041901 (2014)

v_2, v_3, v_4 subtracted

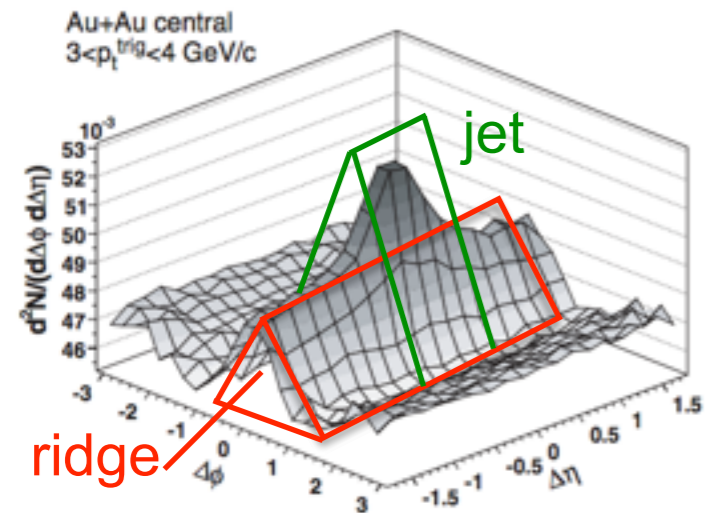
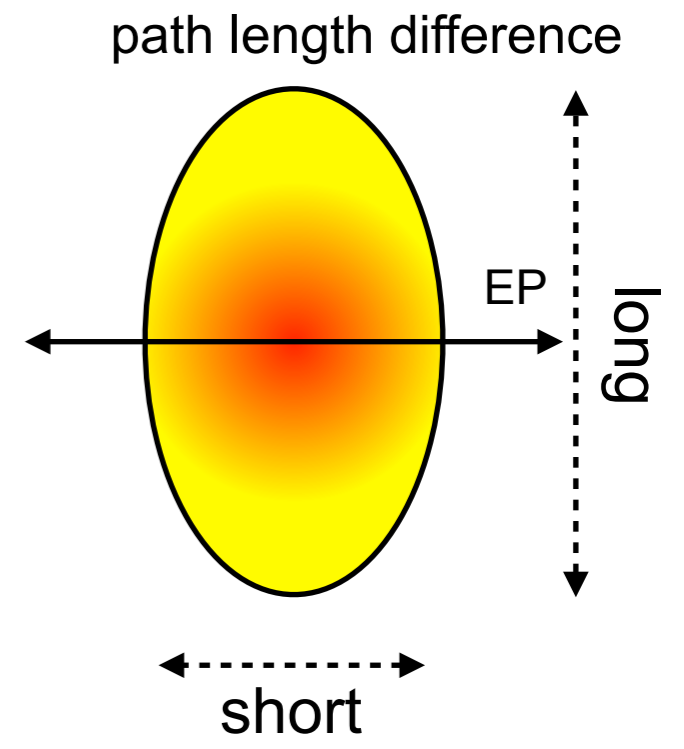
ϕ_s : trigger angle with respect to event plane ($=\phi-\Psi_2$)

in-plane ←

→ out-of-plane



- ◆ Possibility of control in-medium path length of jets
- ◆ EP dependence of jet-medium interactions
 - ▶ Single peak in the away side with the in-plane trigger
 - ▶ Away-side peak becomes lower and broadened as trigger direction changes from in-plane to out-of-plane



Rest of this talk : $|\Delta\eta| < 1$ ► jet cone AND away-side are focused on

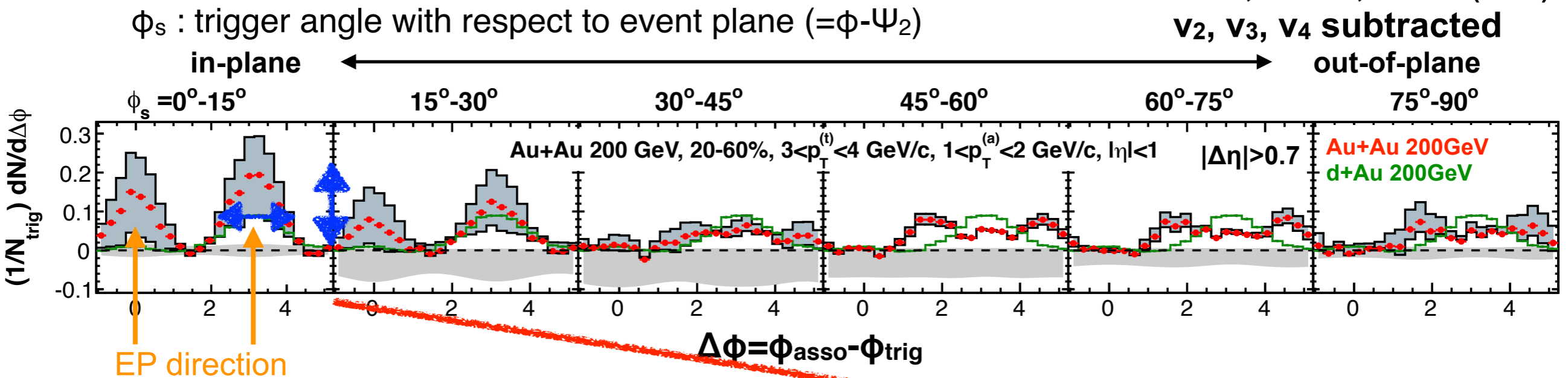
STAR, PRC 80, 064912 (2009)



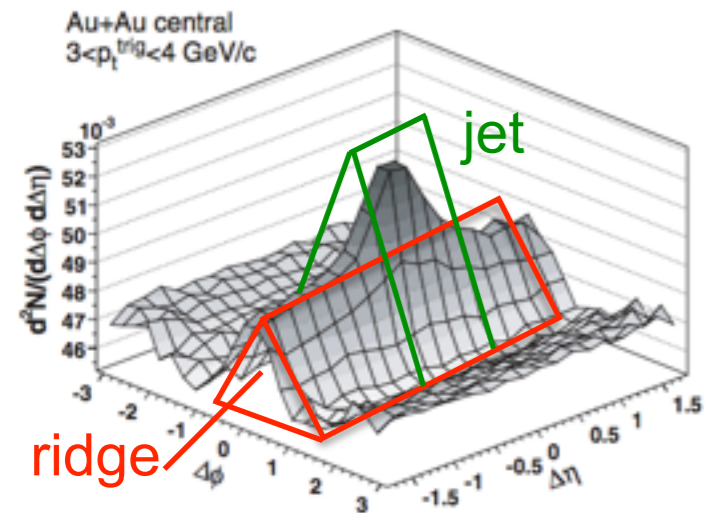
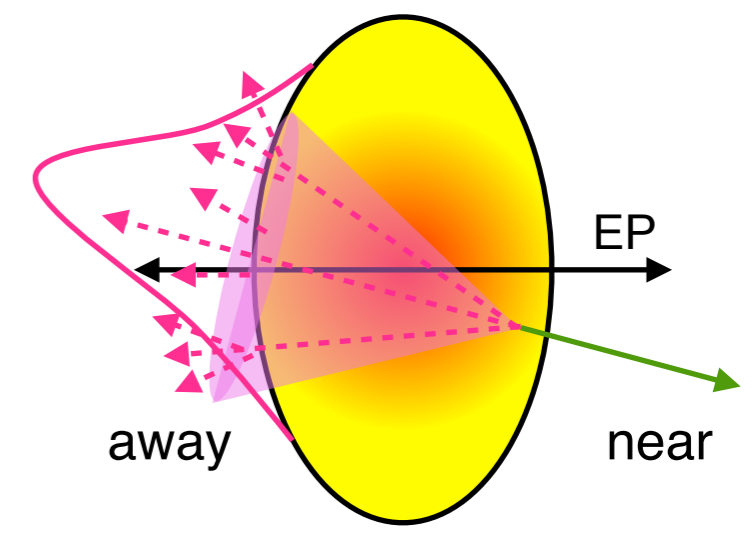
Event plane dependent di-hadron correlations

STAR, PRC 89, 041901 (2014)

v_2, v_3, v_4 subtracted



- ◆ Possibility of control in-medium path length of jets
- ◆ EP dependence of jet-medium interactions
 - ▶ Single peak in the away side with the in-plane trigger
 - ▶ Away-side peak becomes lower and broadened as trigger direction changes from in-plane to out-of-plane



Rest of this talk : $|\Delta\eta| < 1$ ► jet cone AND away-side are focused on

STAR, PRC 80, 064912 (2009)



Event plane dependent di-hadron correlations

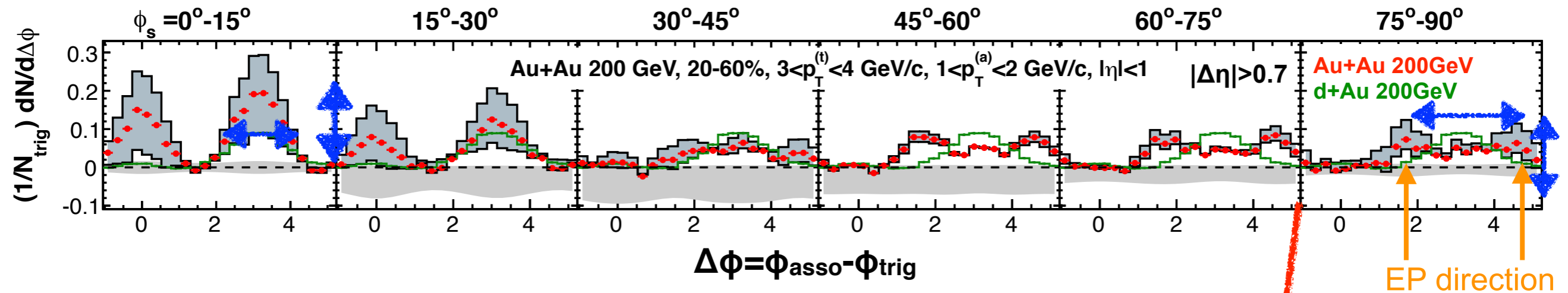
STAR, PRC 89, 041901 (2014)

v_2, v_3, v_4 subtracted

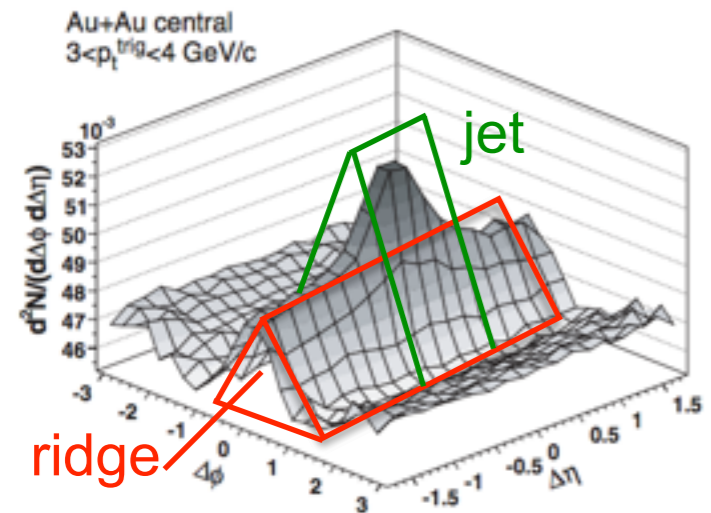
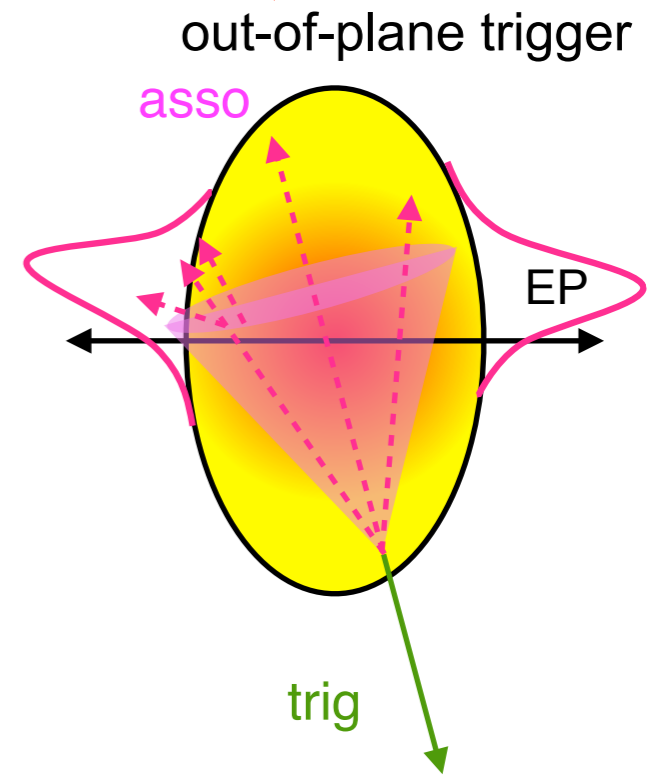
ϕ_s : trigger angle with respect to event plane ($=\phi-\Psi_2$)

in-plane

out-of-plane



- ◆ Possibility of control in-medium path length of jets
- ◆ EP dependence of jet-medium interactions
 - ▶ Single peak in the away side with the in-plane trigger
 - ▶ Away-side peak becomes lower and broadened as trigger direction changes from in-plane to out-of-plane



STAR, PRC 80, 064912 (2009)

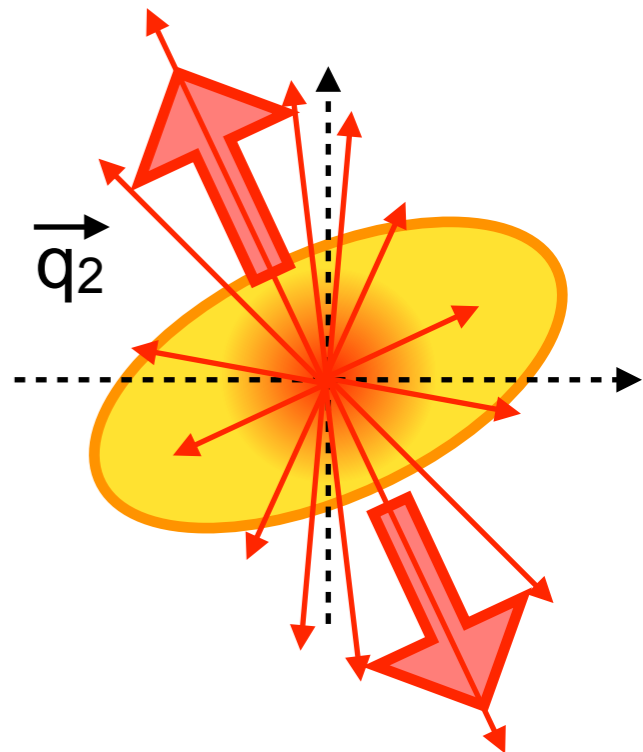
Rest of this talk : $|\Delta\eta| < 1$ ► jet cone AND away-side are focused on



Event shape engineering (ESE)

- ◆ Selection of event-by-event flow amplitude
 - ▶ event-by-event v_2 largely fluctuates in a fixed centrality bin
 - ▶ control fluctuating v_2 by selecting the magnitude of flow vector q_2
 - ▶ Possibility to control the initial geometry

J.Schukraft, A.Timmins and S.A.Voloshin, PLB 719 (2013), 394-398



$$Q_{2,x} = \frac{\sum w_i \cos(2\phi_i)}{\sqrt{\sum w_i}}$$

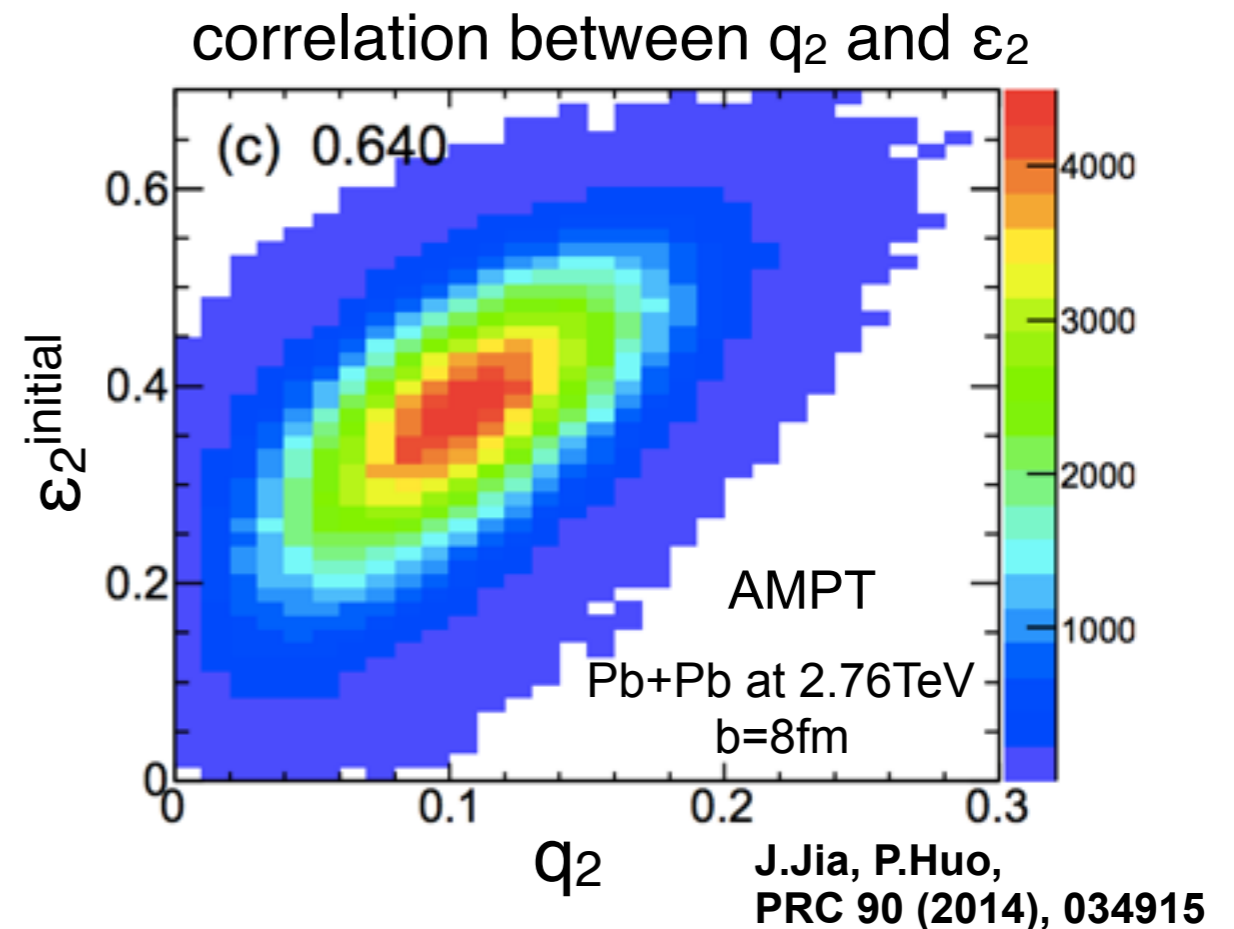
$$Q_{2,y} = \frac{\sum w_i \sin(2\phi_i)}{\sqrt{\sum w_i}}$$

$$q_2 = \sqrt{Q_{2,x}^2 + Q_{2,y}^2}$$

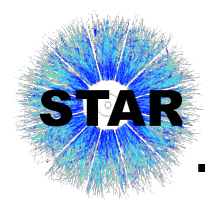
w_i : weighting factor

A.M.Poskanzer, S.A.Voloshin,
PRC 58 (1998), 1671-1678

initial eccentricity $\epsilon_2 = \frac{\langle x^2 - y^2 \rangle}{\langle x^2 + y^2 \rangle}$

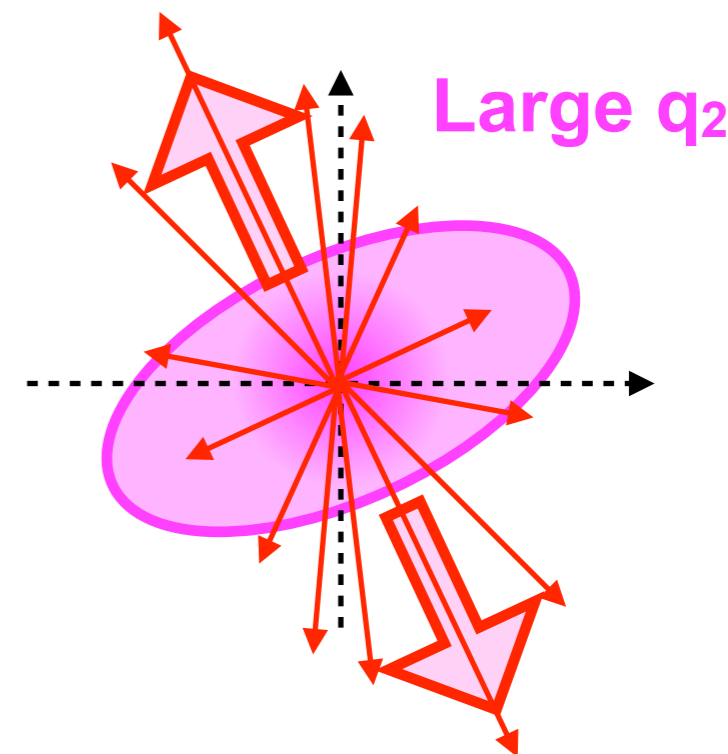
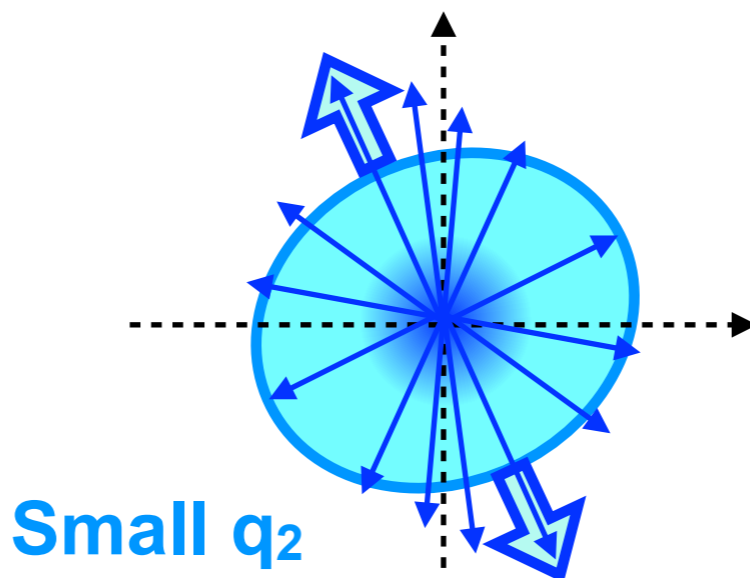
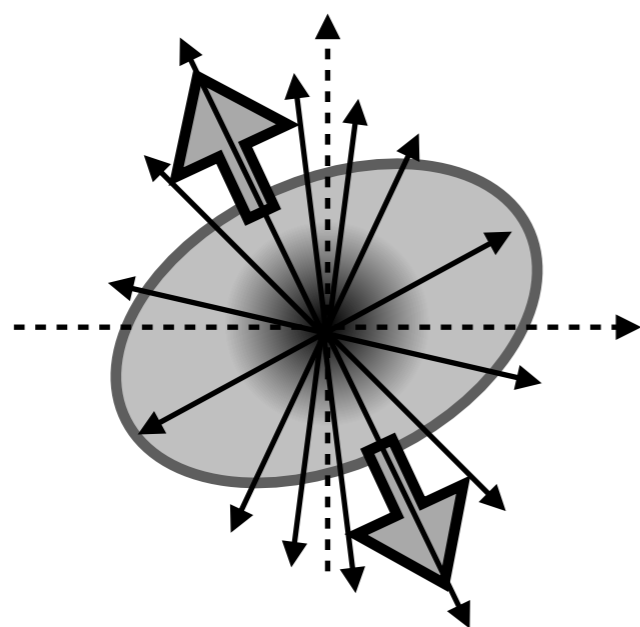


Separation of volume effect and geometry effect could be allowed



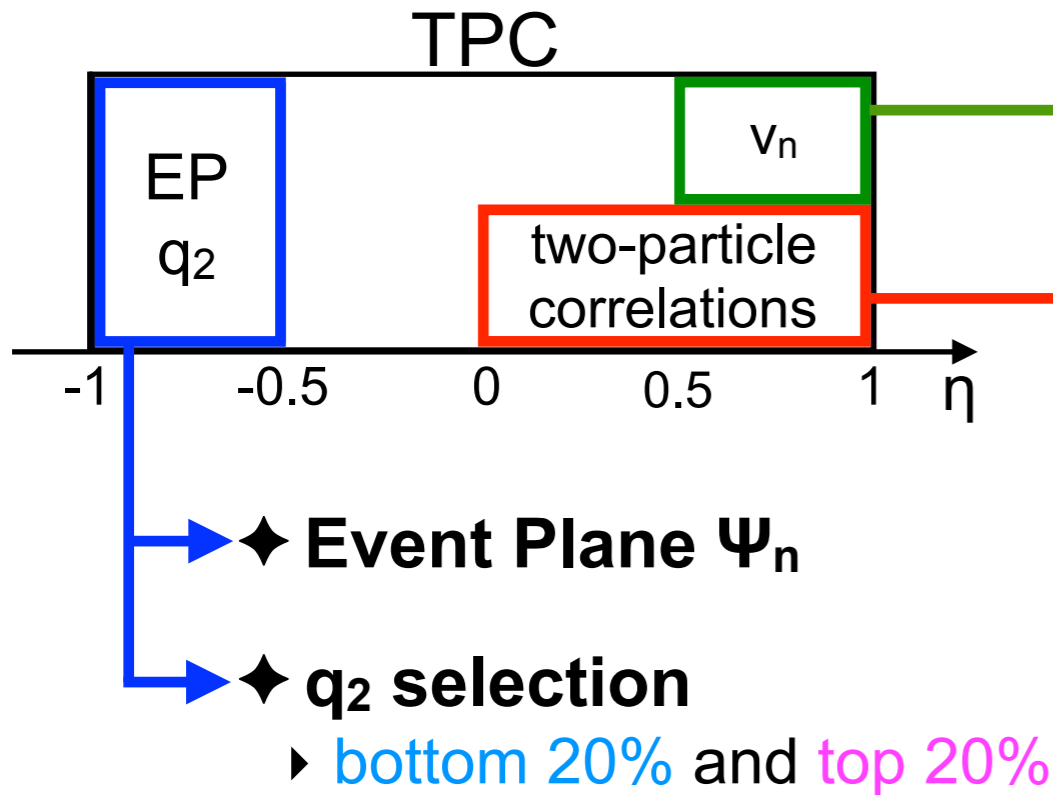
Motivation

- ◆ Combination of **centrality selection** and **event shape engineering** allows control of the initial geometry while keeping the average energy density (multiplicity) fixed
 - ▶ **Study difference of jet modification in medium expansion**
- ◆ Di-hadron correlations with event shape engineering allow new differential insight into energy loss mechanisms as a function of initial energy and shape
 - ▶ **Detailed information which was previously averaged out**
- ◆ **Analysis with minimum-bias Au+Au at $\sqrt{s_{NN}} = 200$ GeV data collected by STAR in 2011**





Data analysis

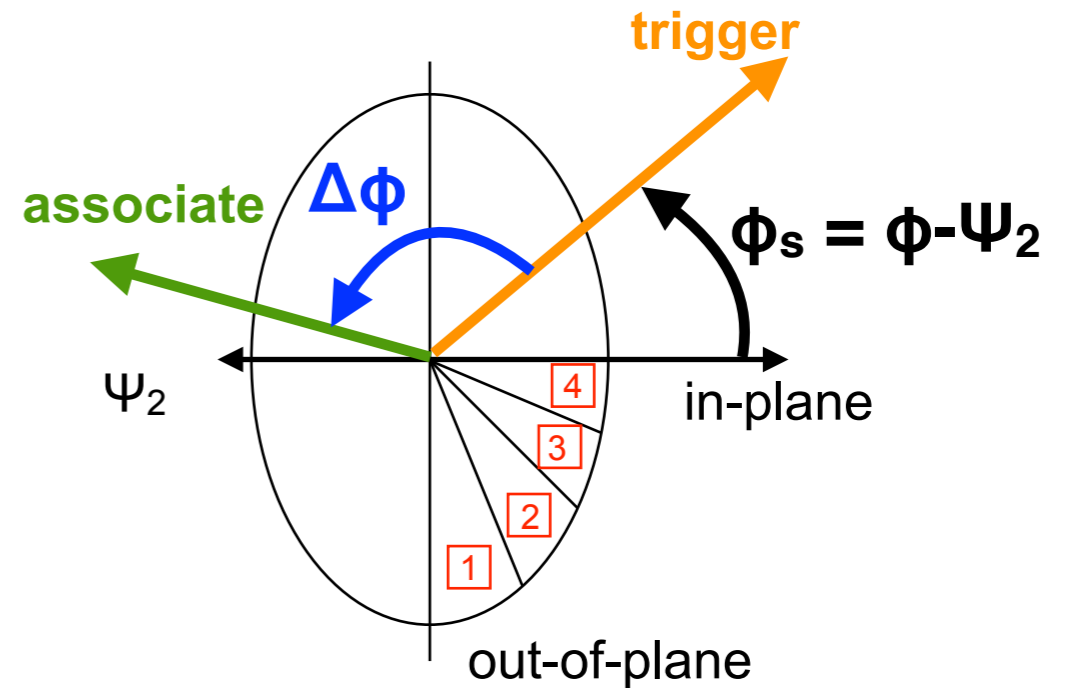
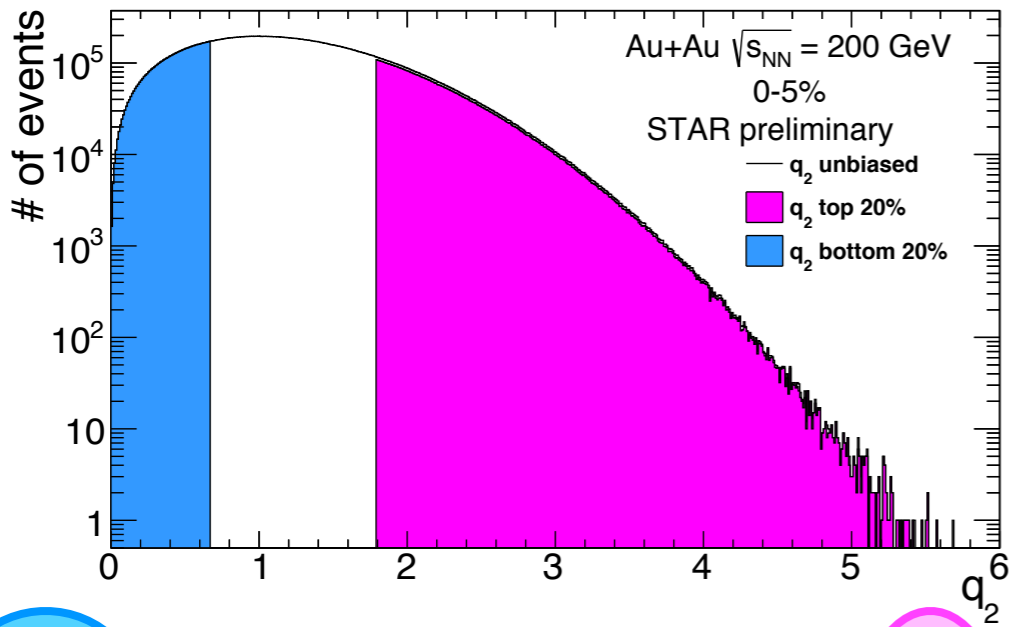


◆ v_n measurement via EP method

◆ Two-particle correlations

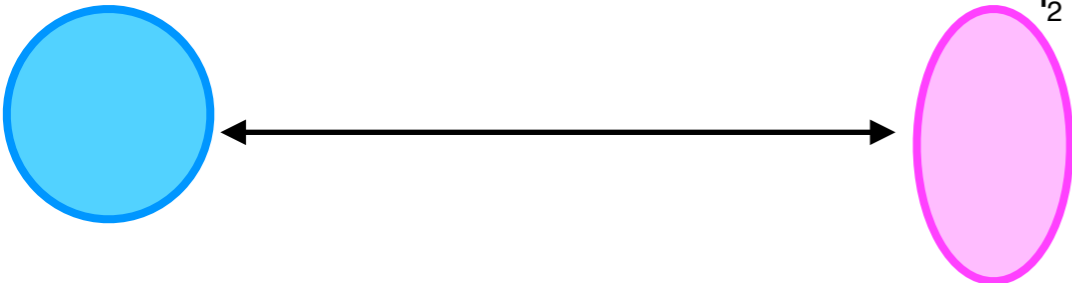
$$C(\Delta\phi) \propto \frac{N_{pair}^{real}(\Delta\phi)}{N_{pair}^{mix}(\Delta\phi)}$$

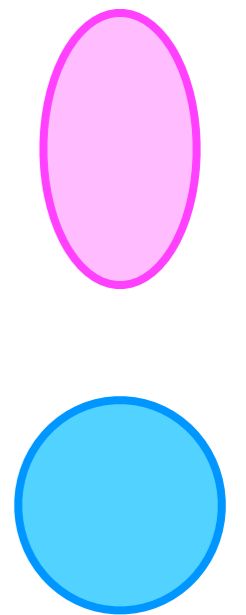
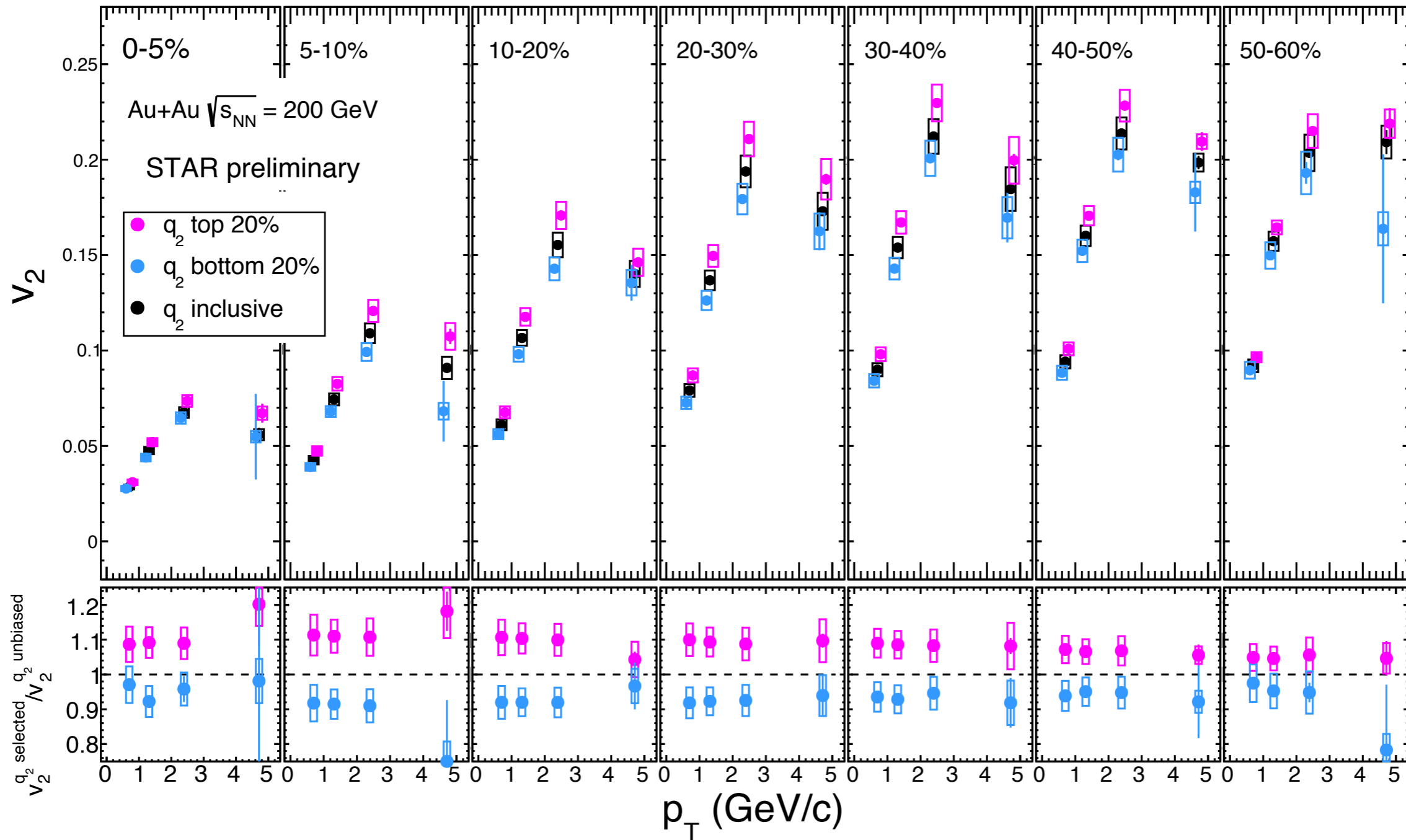
trigger angle selection w.r.t. EP



Background subtraction :

assuming ZYAM with inclusive-triggered correlations and subtract v_2 , v_3 and v_4 contributions





- ◆ v_2 is measured via event plane method with TPC-EP with taking 1.0 η gap
- ◆ 20% largest and smallest q_2 vectors are selected with the same region as TPC-EP
- ◆ Top 20% q_2 selection leads to **~10% larger v_2 events**
- ◆ Bottom 20% q_2 selection leads to **~8% smaller v_2 events**

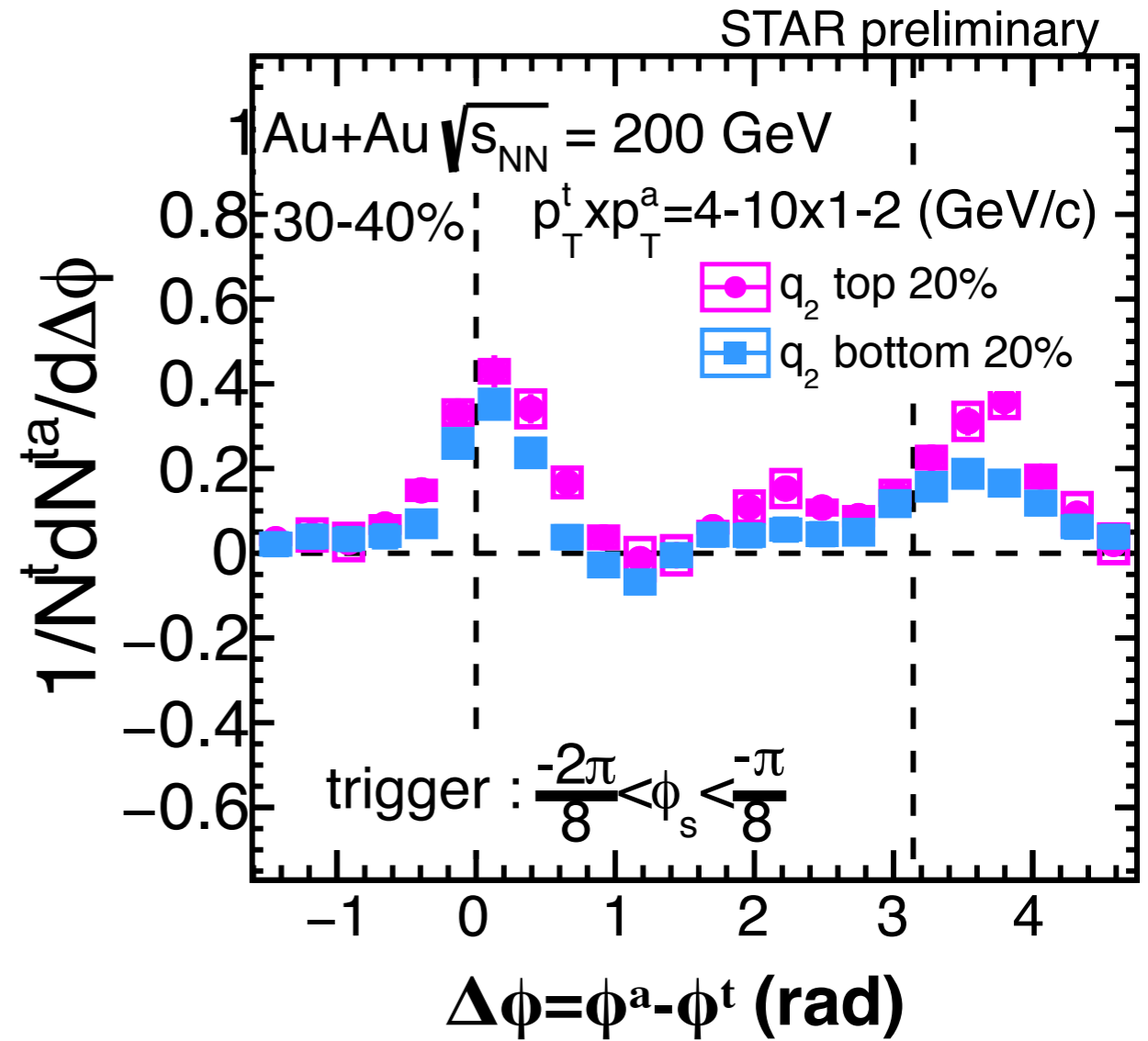
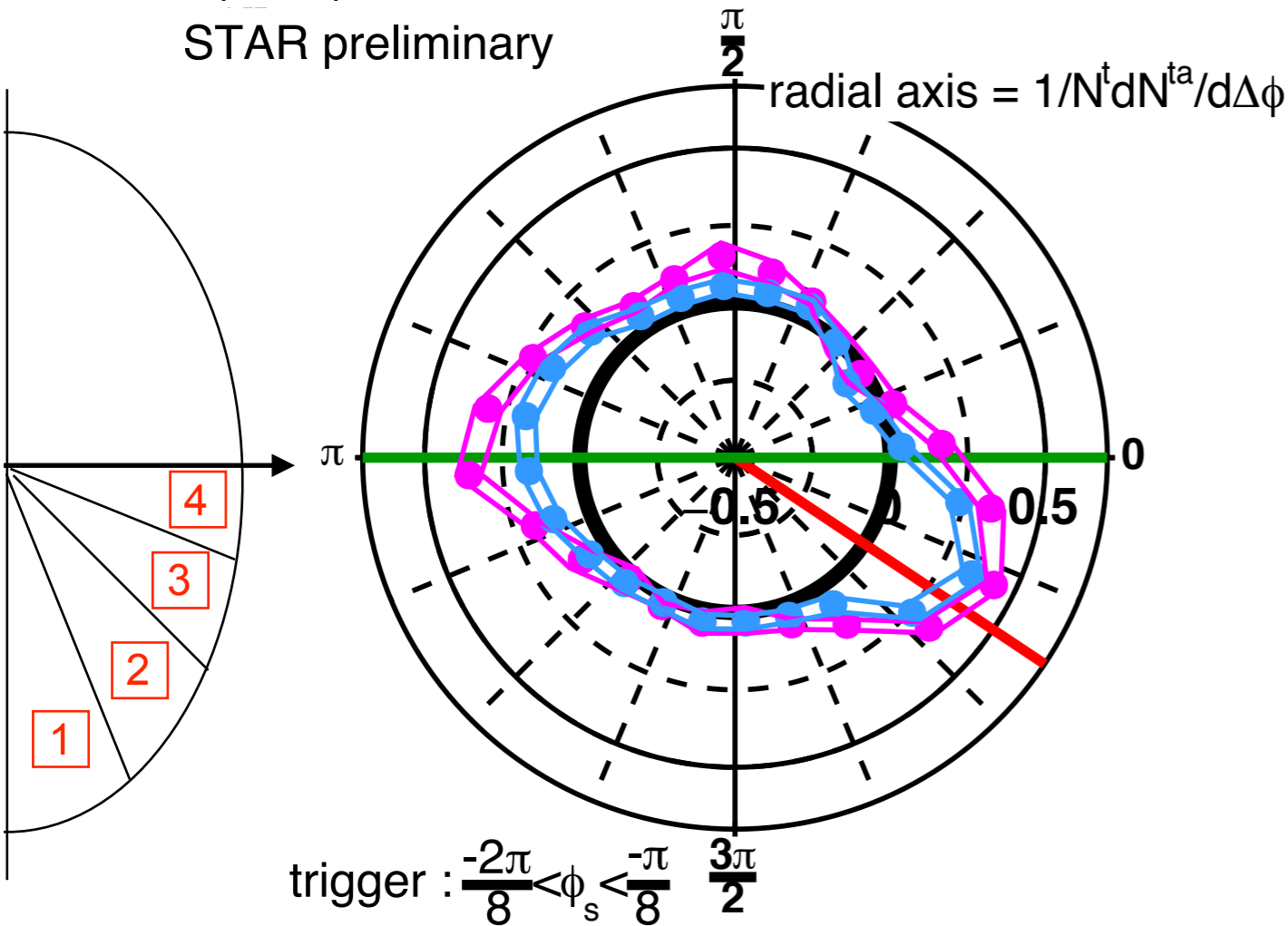


Polar representation of correlated yield

Au+Au $\sqrt{s_{NN}} = 200$ GeV 30-40%

$p_T^t \otimes p_T^a = 4-10 \otimes 1-2$ (GeV/c)

STAR preliminary



- ◆ Two axes should be considered : **back-to-back trigger axis** and **EP axis**
 - Polar representations are displayed so that the correlation shapes are visually clear
- ◆ Relative angle $\Delta\phi$ starts from **red line** and rotate toward counter-clockwise direction
- ◆ The amplitudes of correlated yield correspond to the radius

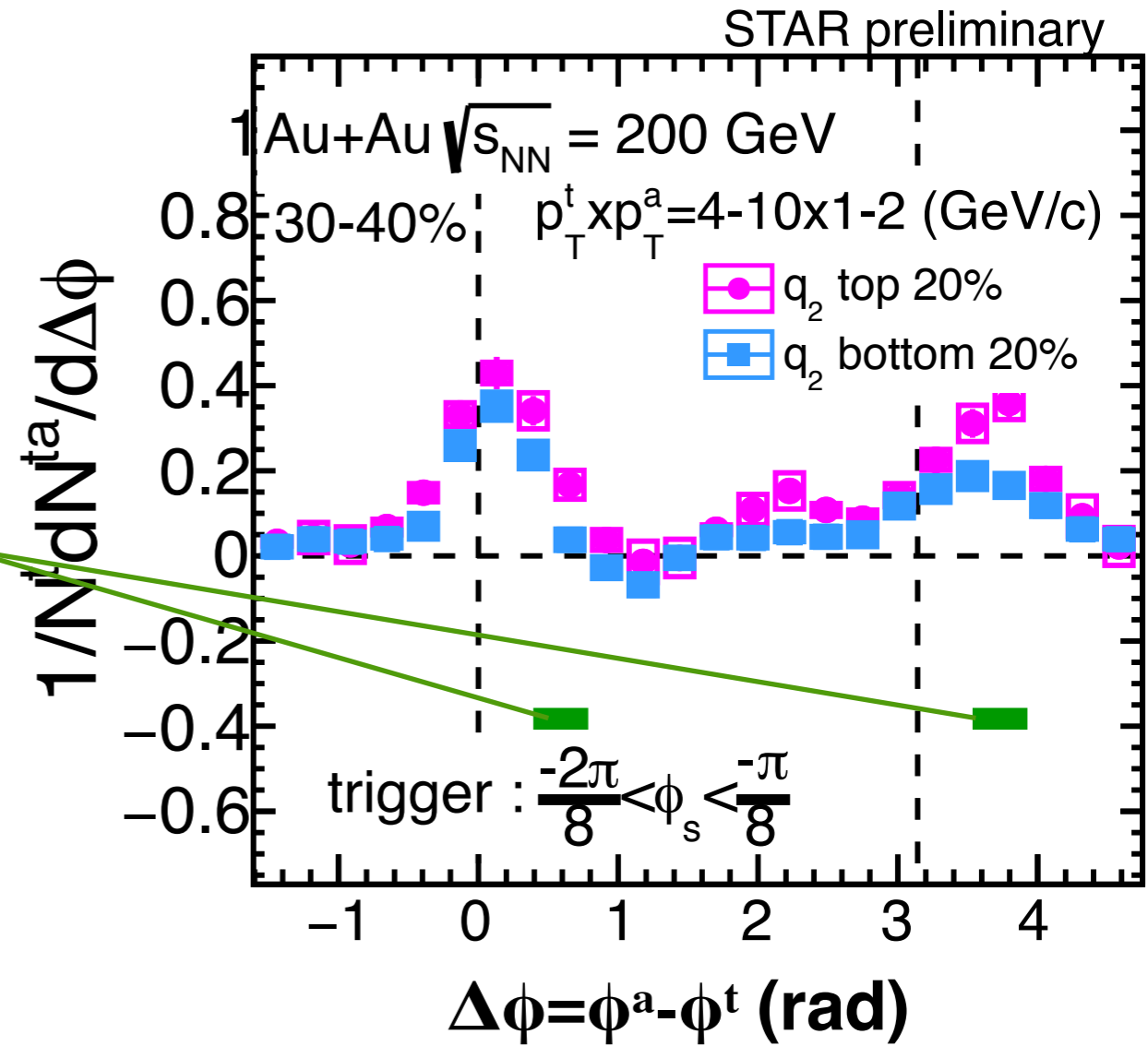
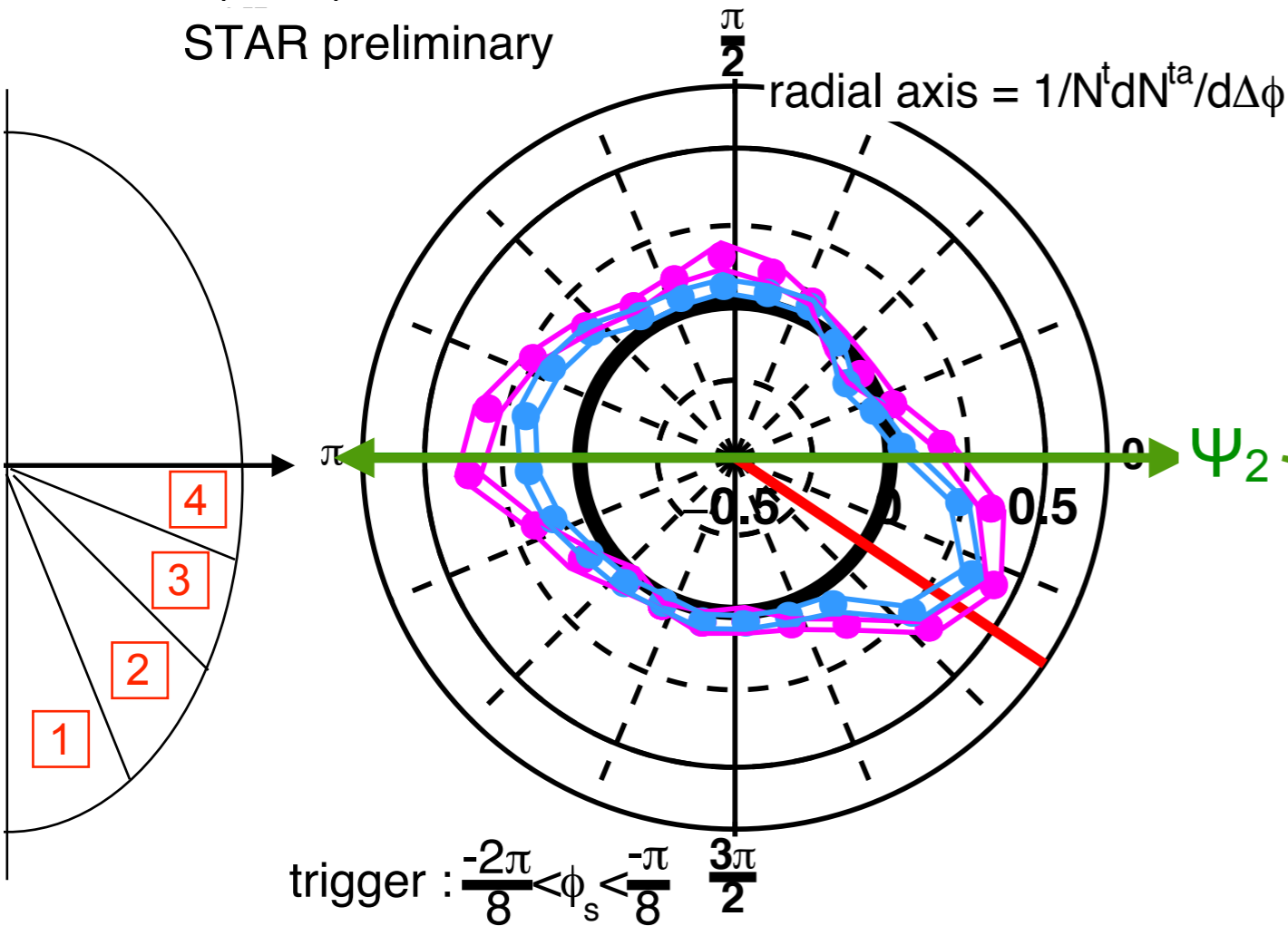


Polar representation of correlated yield

Au+Au $\sqrt{s_{NN}} = 200$ GeV 30-40%

$p_T^t \otimes p_T^a = 4-10 \otimes 1-2$ (GeV/c)

STAR preliminary



- ◆ Two axes should be considered : **back-to-back trigger axis** and **EP axis**
 - Polar representations are displayed so that the correlation shapes are visually clear
- ◆ Relative angle $\Delta\phi$ starts from **red line** and rotate toward counter-clockwise direction
- ◆ The amplitudes of correlated yield correspond to the radius

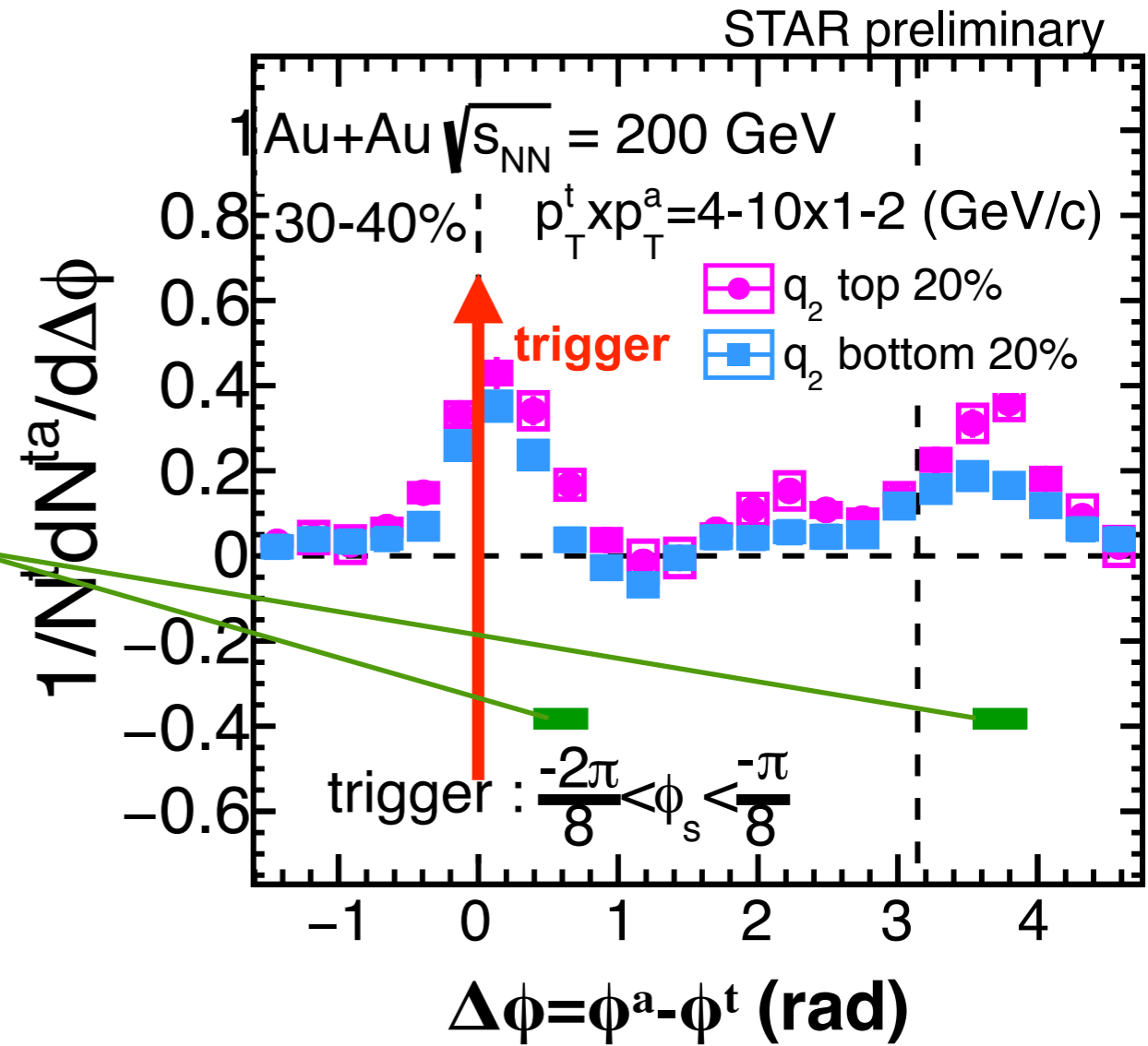
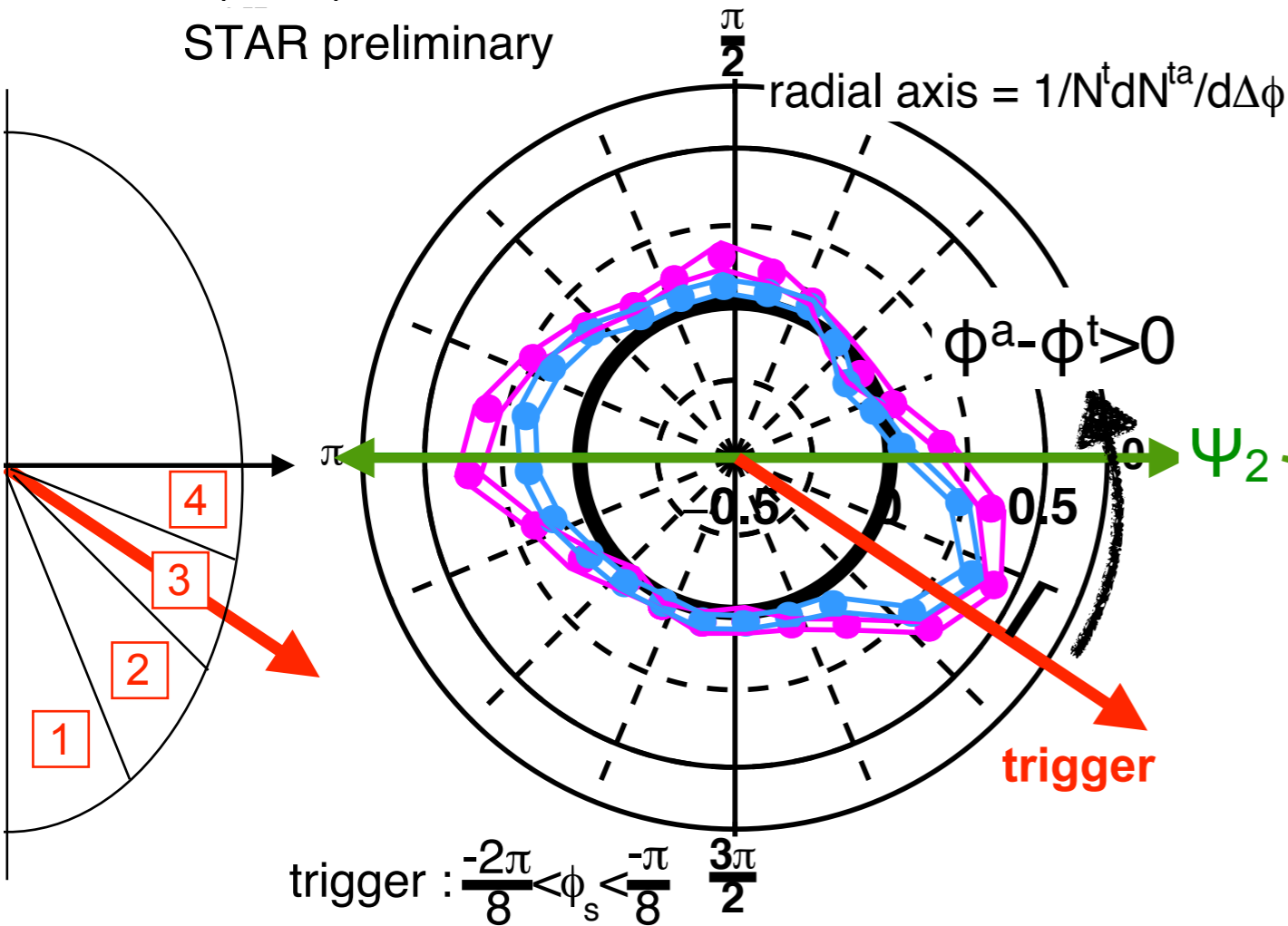


Polar representation of correlated yield

Au+Au $\sqrt{s_{NN}} = 200$ GeV 30-40%

$p_T^t \otimes p_T^a = 4-10 \otimes 1-2$ (GeV/c)

STAR preliminary



- ◆ Two axes should be considered : **back-to-back trigger axis** and **EP axis**
 - Polar representations are displayed so that the correlation shapes are visually clear
- ◆ Relative angle $\Delta\phi$ starts from **red line** and rotate toward counter-clockwise direction
- ◆ The amplitudes of correlated yield correspond to the radius

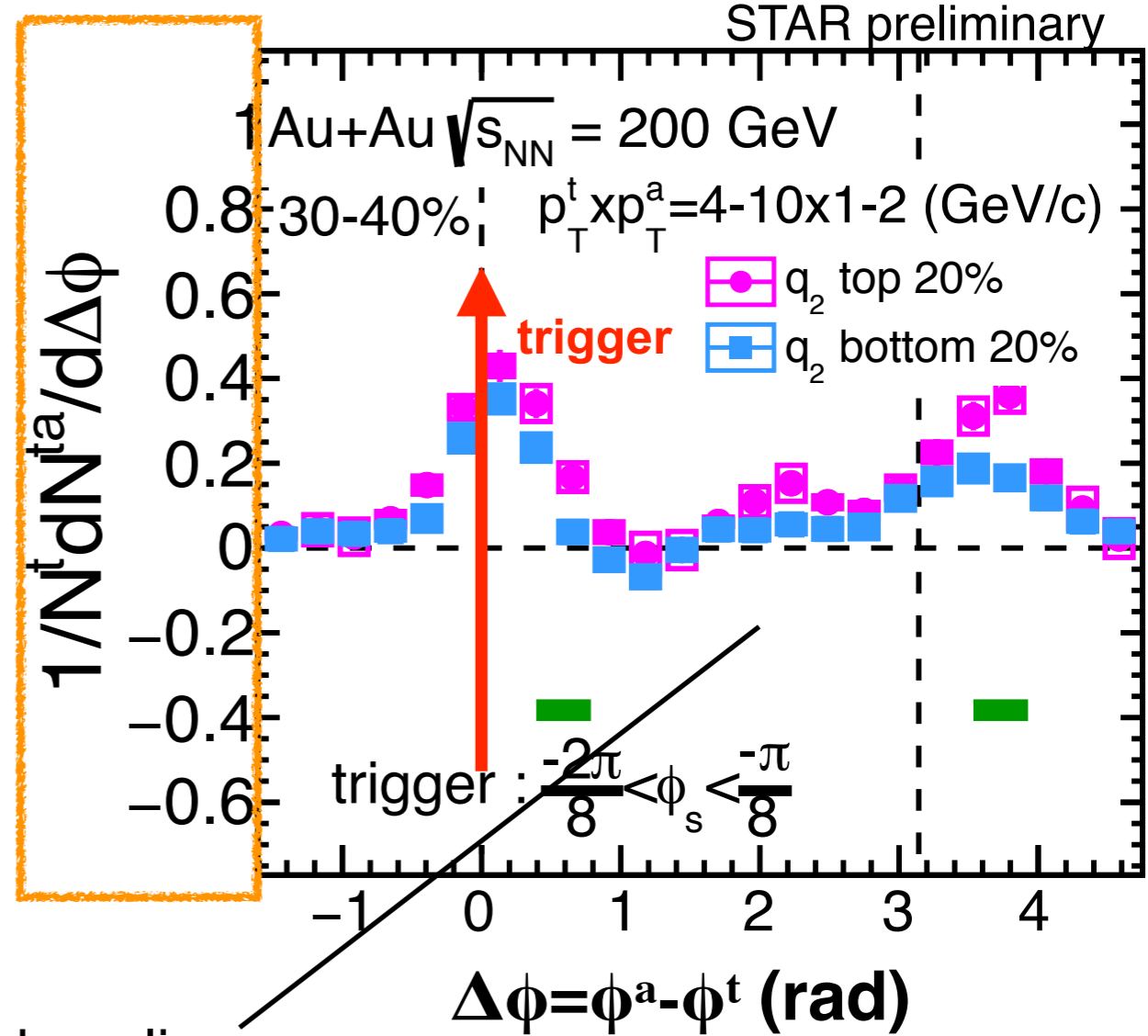
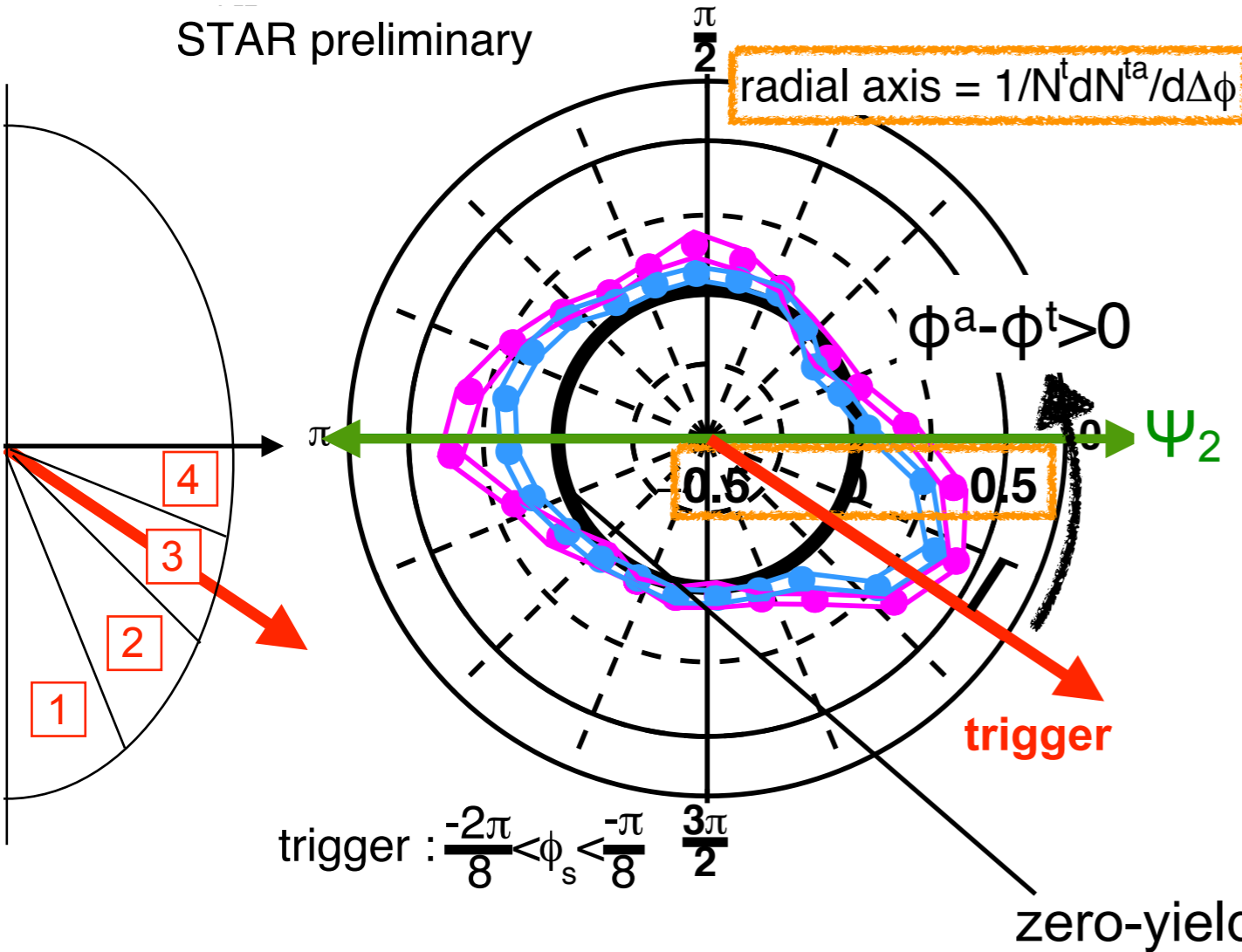


Polar representation of correlated yield

Au+Au $\sqrt{s_{NN}} = 200$ GeV 30-40%

$p_T^t \otimes p_T^a = 4-10 \otimes 1-2$ (GeV/c)

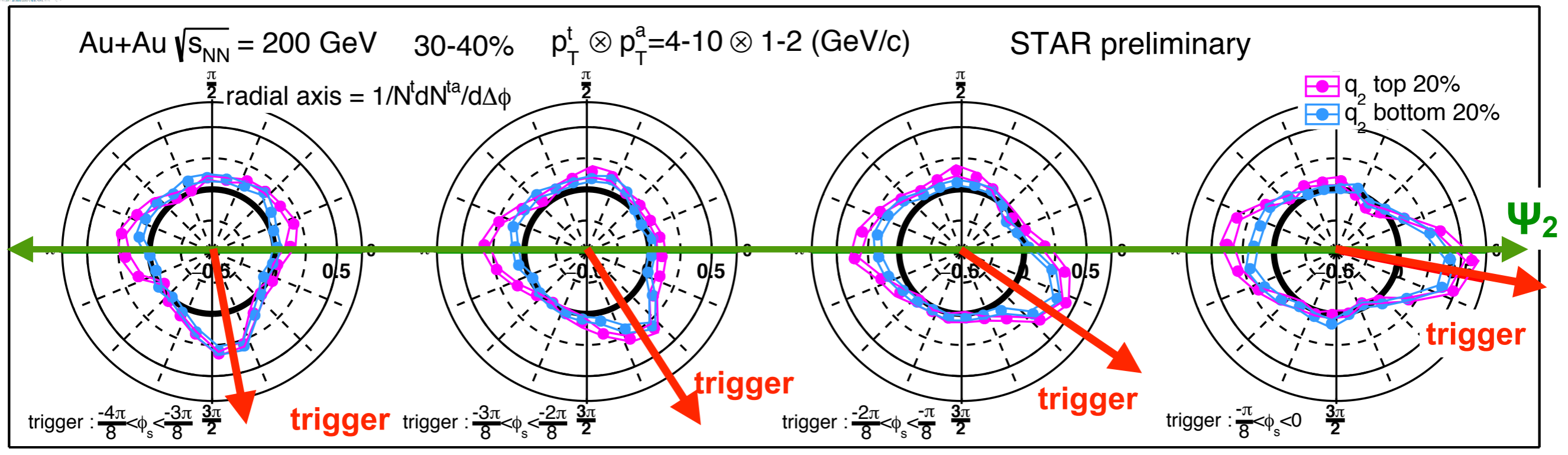
STAR preliminary



- ◆ Two axes should be considered : **back-to-back trigger axis** and **EP axis**
 - Polar representations are displayed so that the correlation shapes are visually clear
- ◆ Relative angle $\Delta\phi$ starts from **red line** and rotate toward counter-clockwise direction
- ◆ The amplitudes of correlated yield correspond to the radius



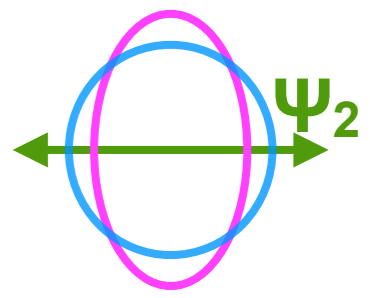
Trigger angle dependence



out-of-plane trigger \longleftrightarrow in-plane trigger

◆ Near side

- ▶ No difference between large- q_2 and small- q_2 events with trigger out-of-plane
- ▶ Peak height is enhanced with going to in-plane trigger
 - ▶ The enhancement is larger in large- q_2 events



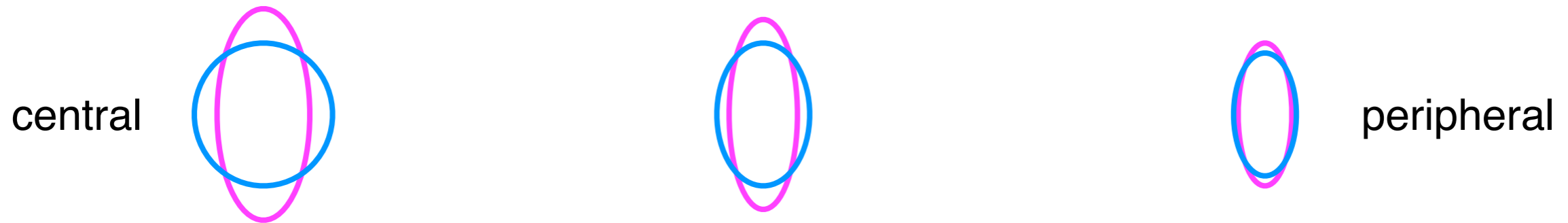
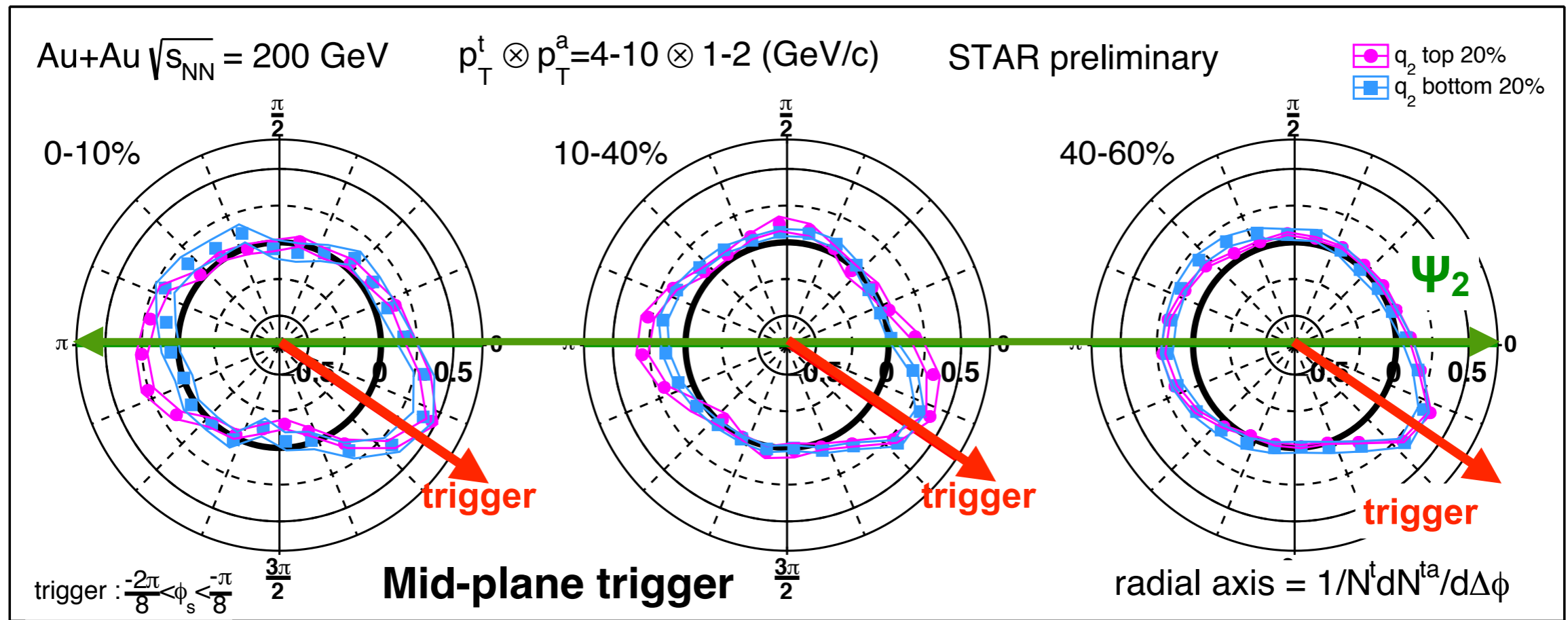
◆ Away side

- ▶ Peak is almost fully suppressed with trigger out-of-plane both in large- q_2 and small- q_2 events and remnant yield in the EP direction has q_2 dependence
- ▶ Peak height is enhanced with going to in-plane trigger

➔ Low- p_T particles preferentially escape toward in-plane direction?

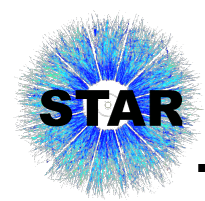


Centrality dependence



- ◆ See how shifting of away-side peak depends on centrality and q_2
- ◆ Larger shift in large q_2 events
- ◆ q_2 dependence is stronger in central events
- ◆ No q_2 dependence in peripheral events

➡ Related to path-length or initial eccentricity?



Summary

- ◆ **Di-hadron correlations with respect to the event plane with event shape engineering at the STAR experiment**
 - ▶ Separation between **large- q_2** and **small- q_2** events enhances difference of correlation shape while preserving average multiplicity in central and mid-central collisions
 - ➔ new handle to differentially study partonic energy loss mechanisms

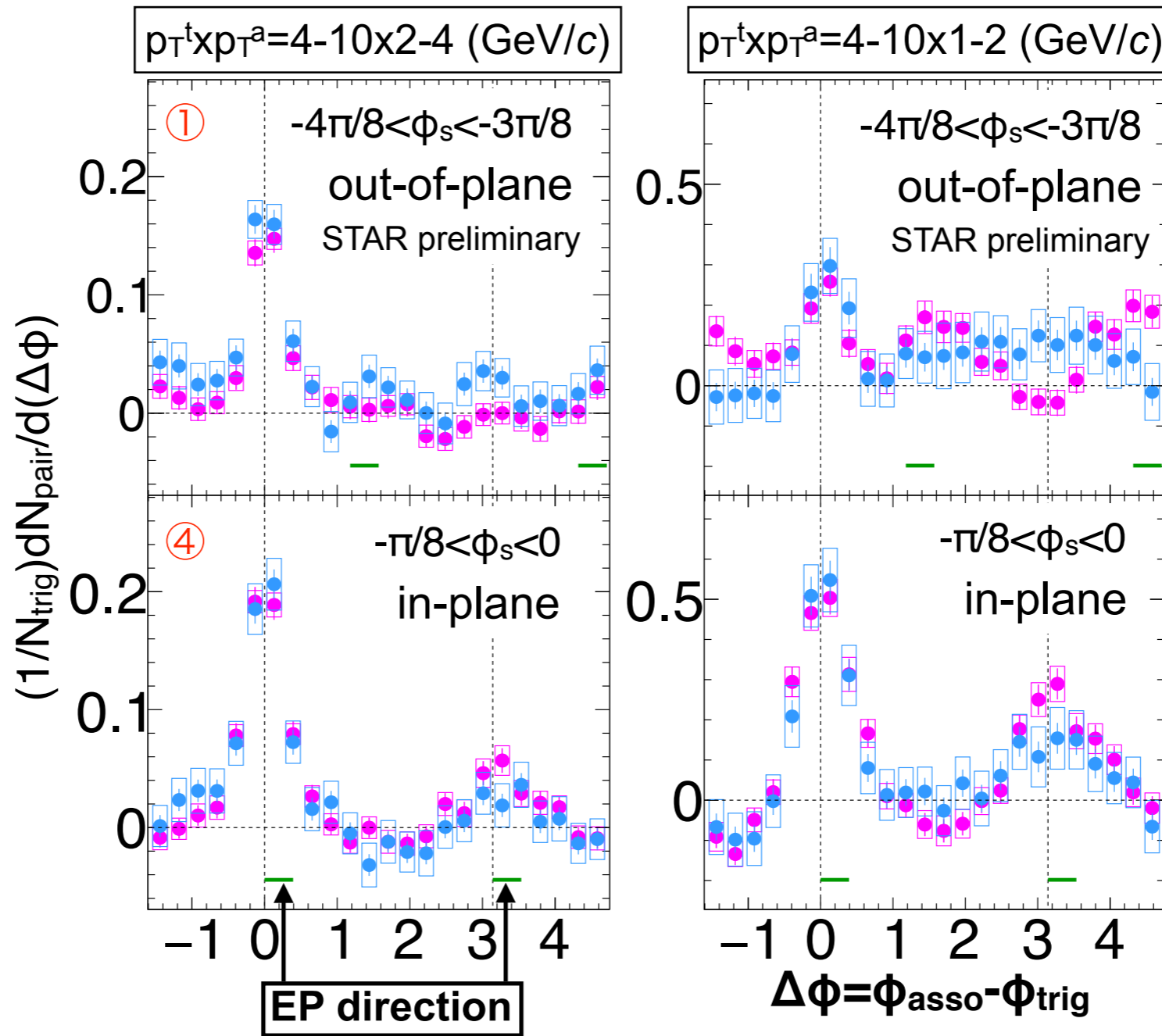
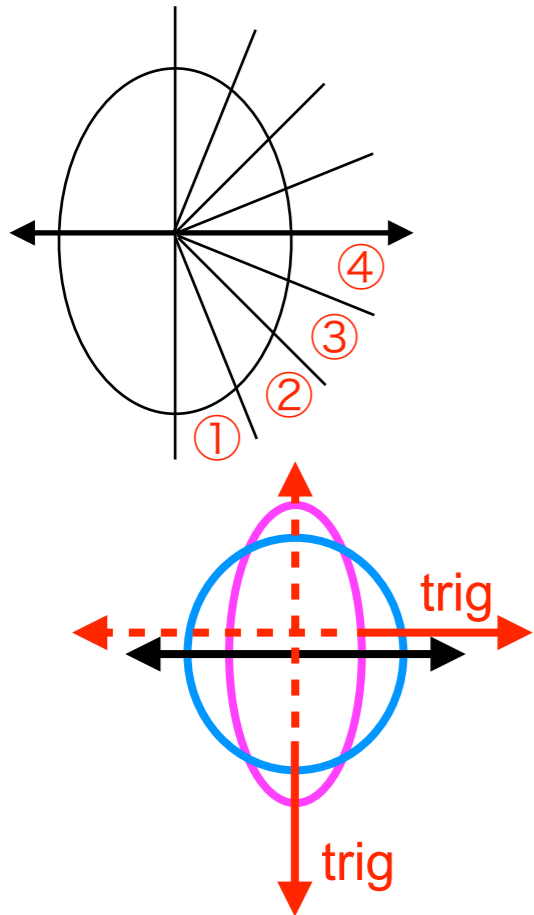
- ◆ **Future work**
 - ▶ Near- and away-side structure will be quantitatively discussed
 - ▶ Experimental results will be compared with some models

Back up



Correlations with q_2 selection

Au+Au $\sqrt{s_{NN}} = 200$ GeV
 0-10%
 ● q_2 top 20%
 ● q_2 bottom 20%

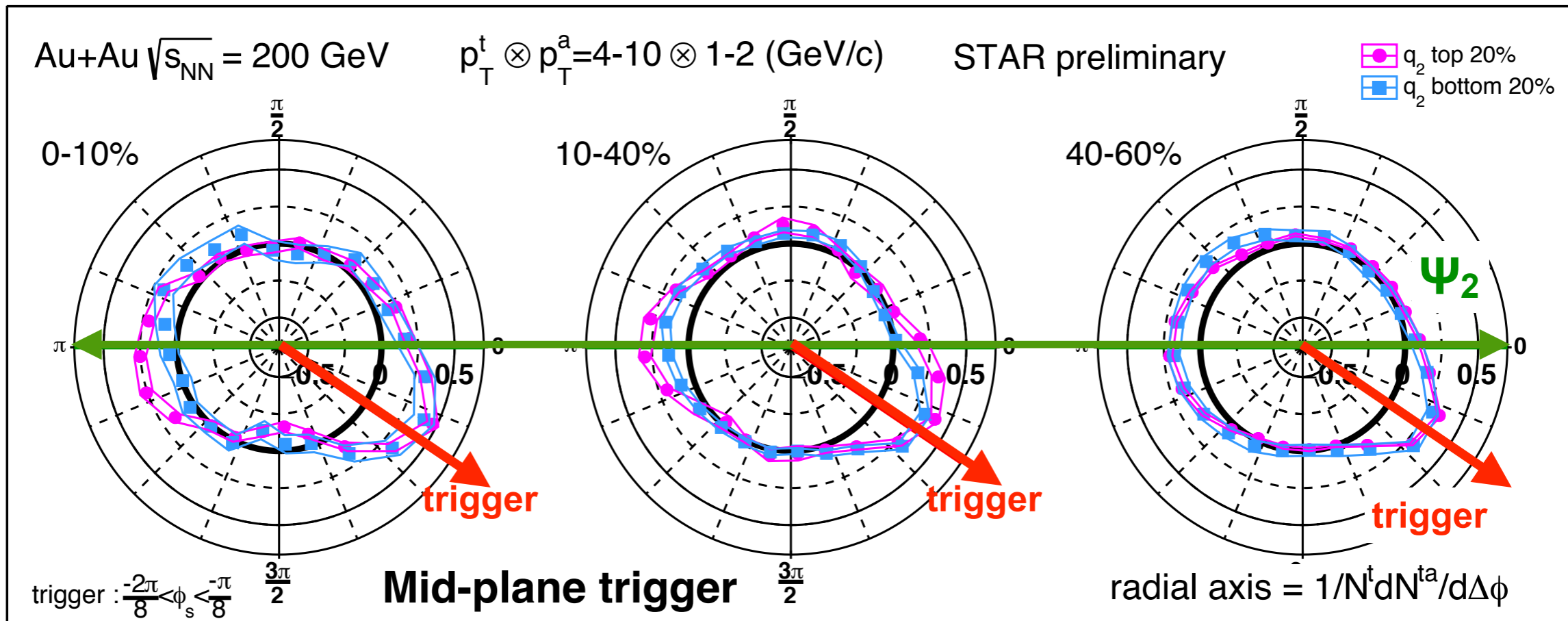
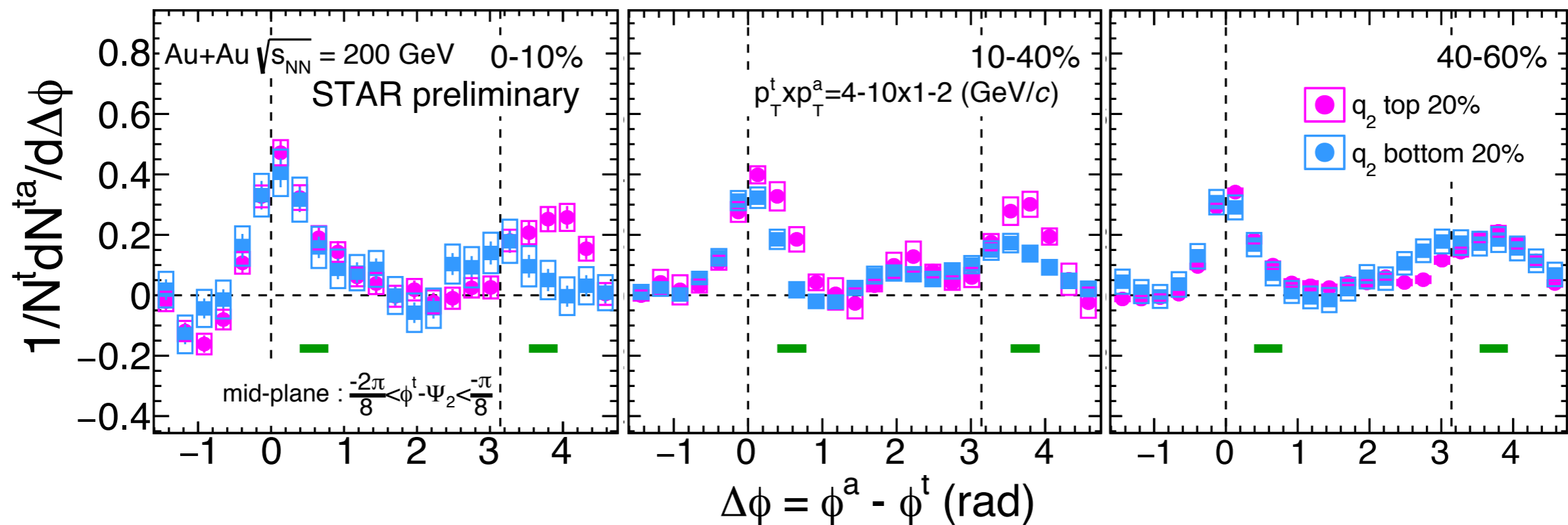


- ◆ High- p_T particles penetrate more with short path length
- ◆ Low- p_T particles are pushed toward in-plane direction and this effect is stronger in large q_2

➡ path-length dependent yield on the away side

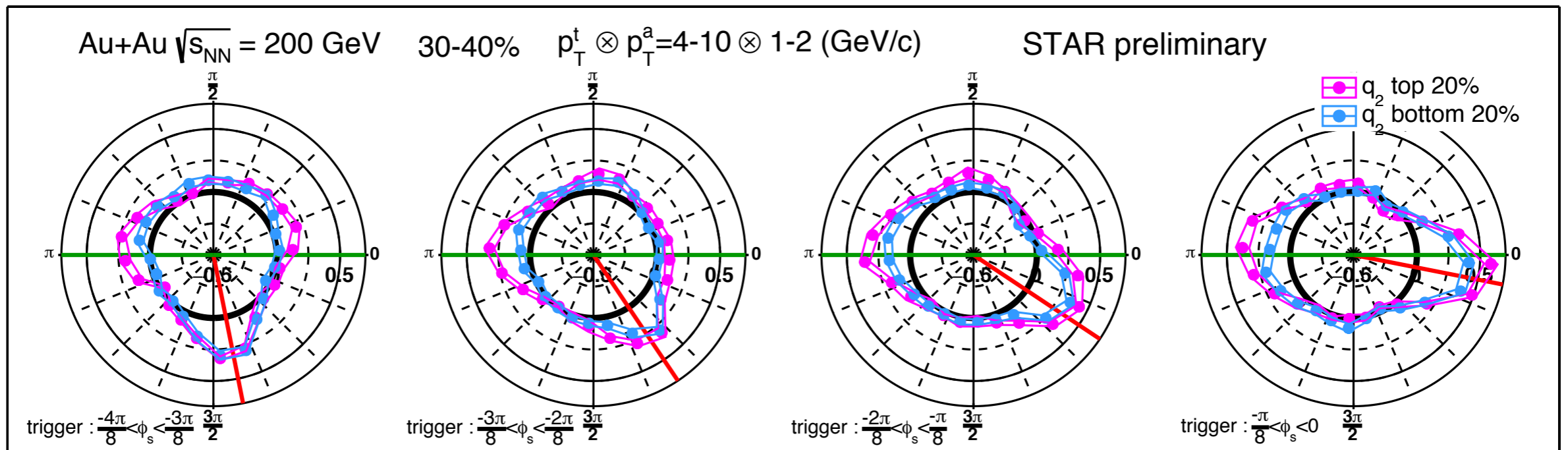
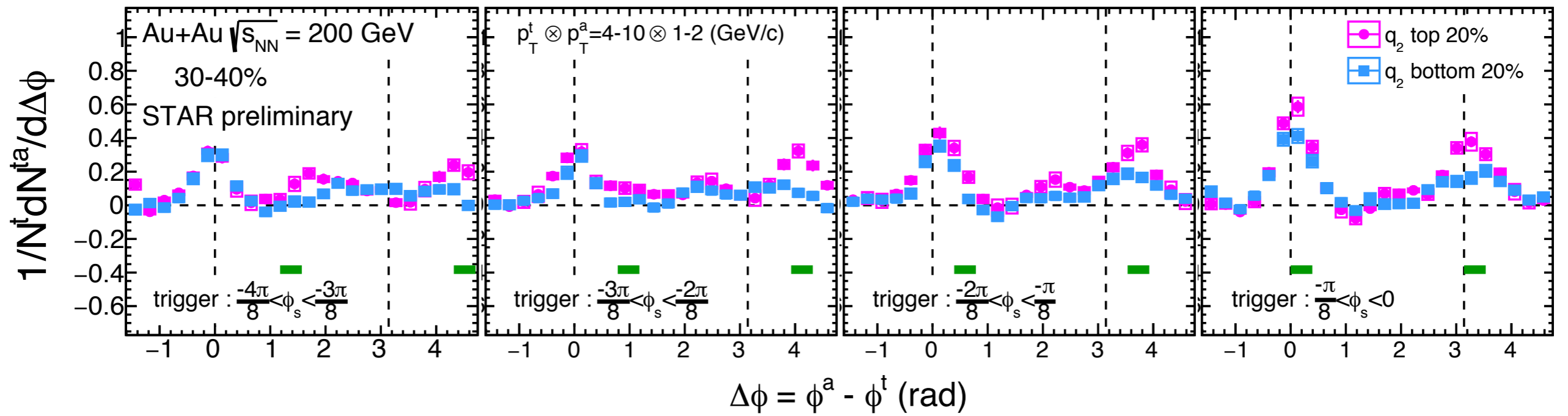


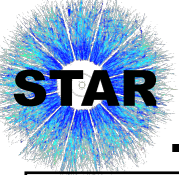
Comparison of polar and traditional distributions





Comparison of polar and traditional distributions

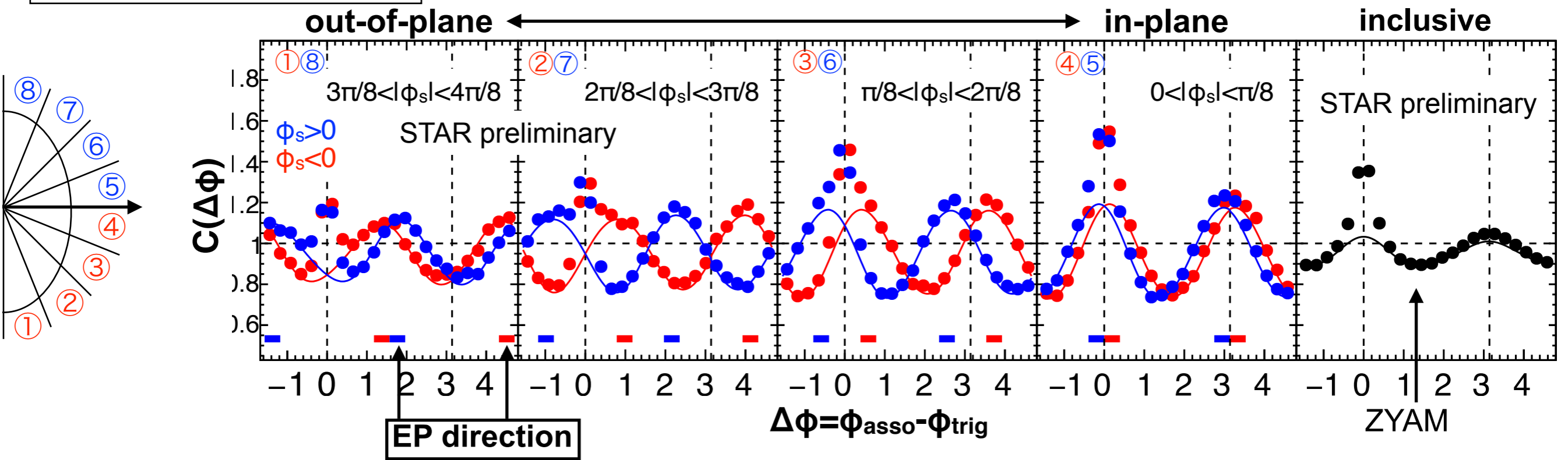




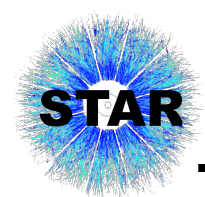
Correlations before flow subtraction and EP correction

Au+Au $\sqrt{s_{NN}} = 200$ GeV
 20-30%, w/o q_2 selection
 $p_T^t \times p_T^a = 4-10 \times 2-4$ (GeV/c)

● raw data
 — background function ($v_2 \oplus v_3 \oplus v_4$)



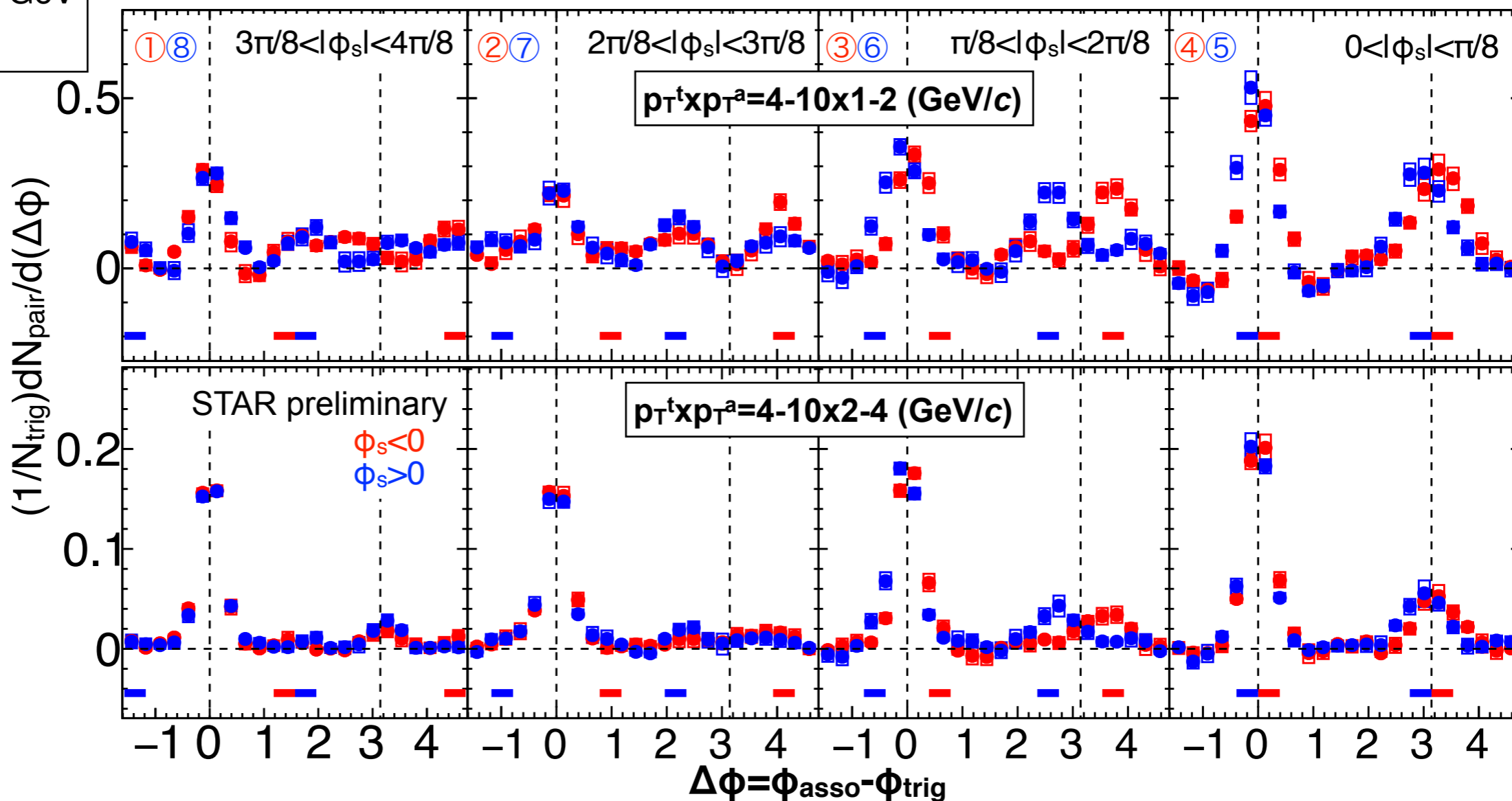
- ◆ Correlation shape
 - ▶ Left/Right mirror symmetric trigger selection w.r.t. EP leads to **mirror-imaged distributions** on the away side
- ◆ Flow background subtraction
 - ▶ Background **shape** is determined by data-driven simulation
 - ▶ Background **level** is determined by inclusive trigger data with ZYAM assumption
- ◆ Correction of trigger smearing effect
 - ▶ Smearing of trigger particle's angle due to limited EP resolution is corrected with unfolding method after flow subtraction



Correlations after flow subtraction and EP correction

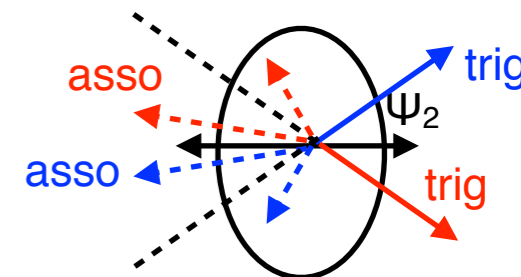
Au+Au $\sqrt{s_{NN}} = 200$ GeV
10-40%

out-of-plane ← → in-plane



- ◆ Amplitudes increase as going to in-plane trigger on both near and away side
- ◆ Left/Right separation leads to asymmetric path length
 - ▶ averaged out in the previous measurement
- ◆ Away-side particles pushed toward in-plane direction

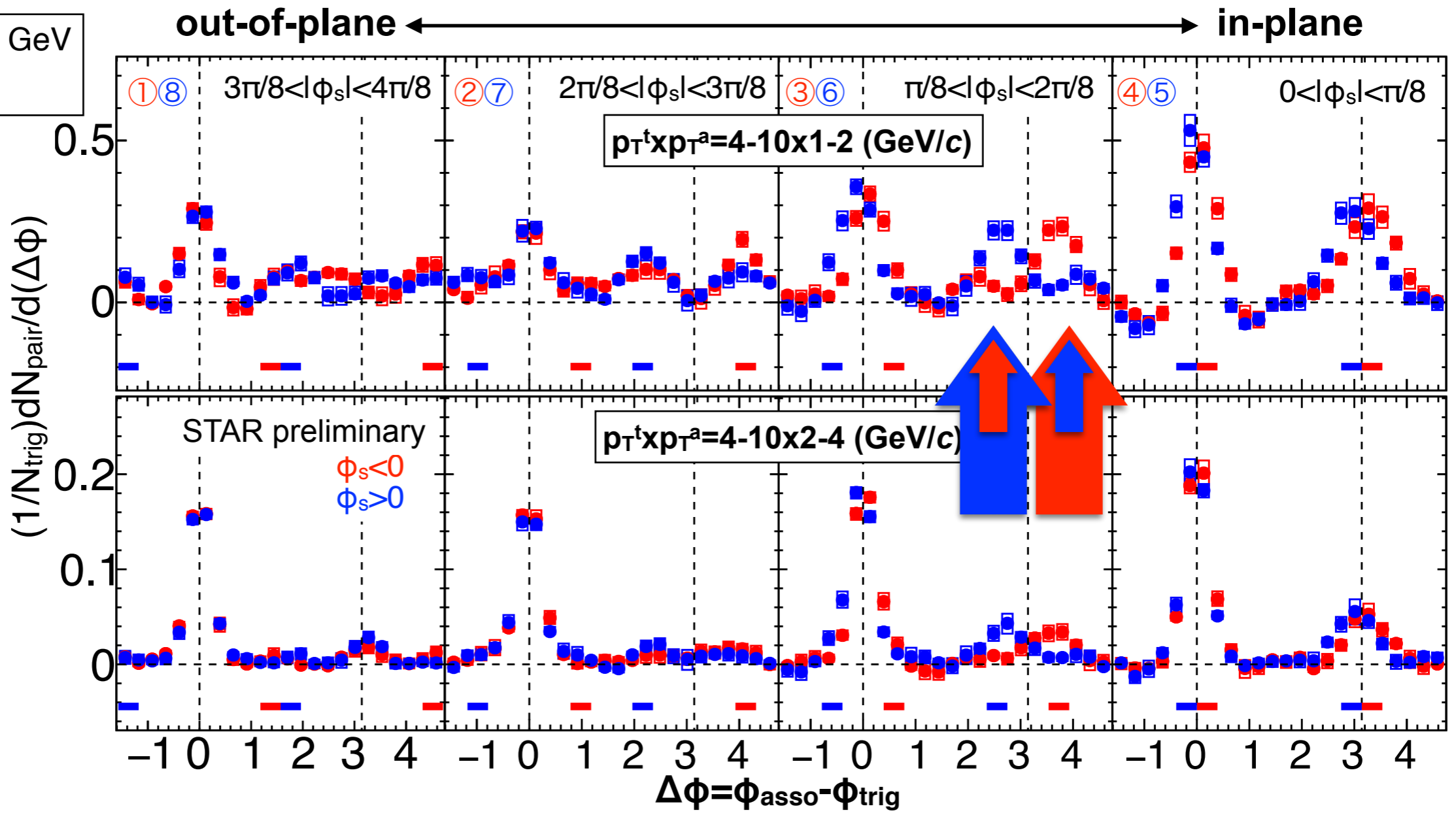
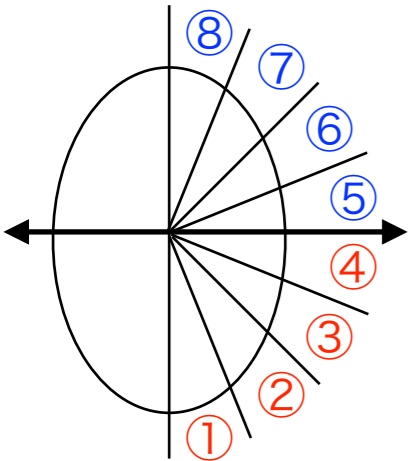
▶ path-length dependent jet modification



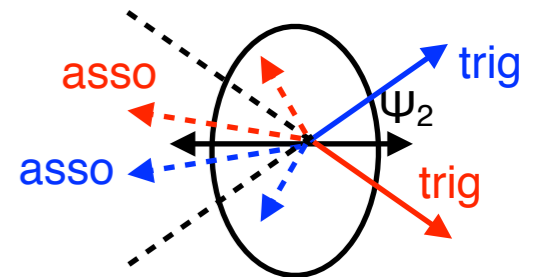


Correlations after flow subtraction and EP correction

Au+Au $\sqrt{s_{NN}} = 200$ GeV
10-40%



- ◆ Amplitudes increase as going to in-plane trigger on both near and away side
- ◆ Left/Right separation leads to asymmetric path length
 - ▶ averaged out in the previous measurement
- ◆ Away-side particles pushed toward in-plane direction

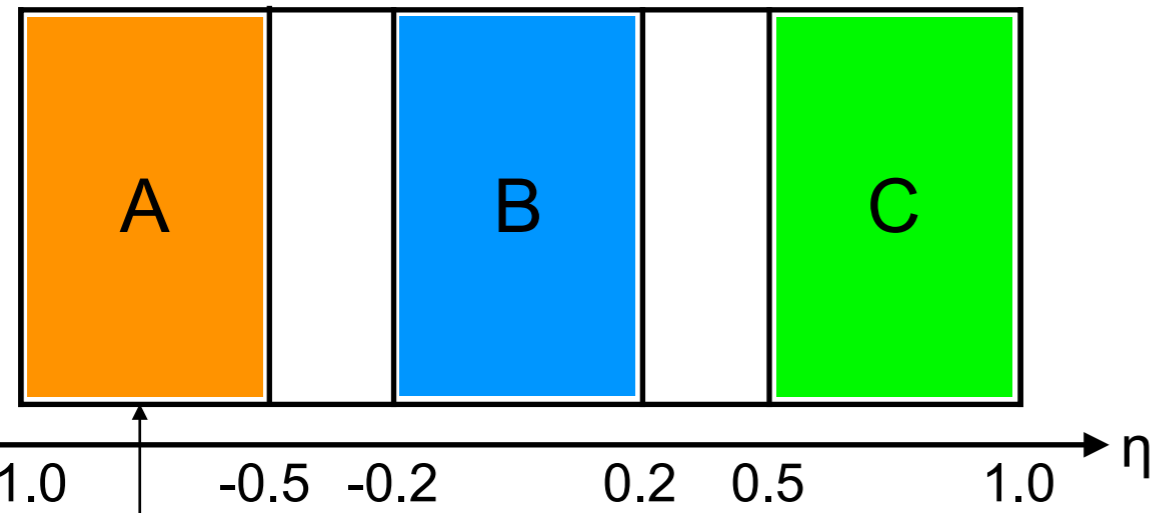
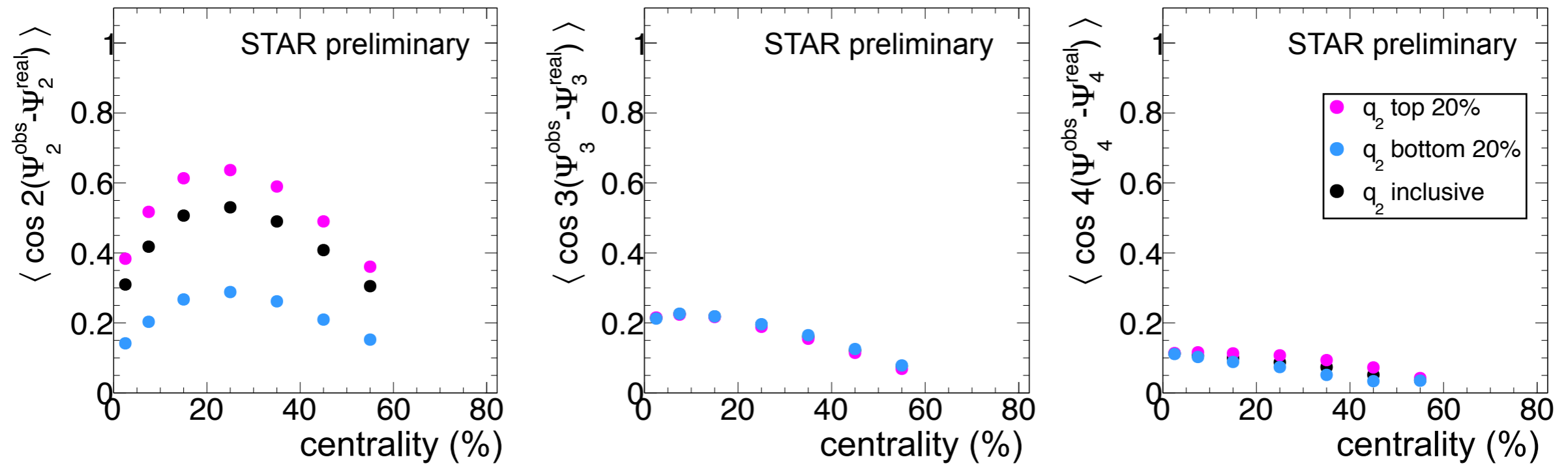


▶ path-length dependent jet modification



Resolution of EP

Au+Au $\sqrt{s_{NN}} = 200$ GeV

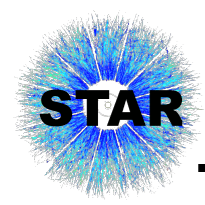


EP determination
q₂ selection

EP resolution via 3 sub-event method

$$\text{Res}\{\Psi_n^A\} = \sqrt{\frac{\langle \cos n(\Psi_n^A - \Psi_n^B) \rangle \langle \cos n(\Psi_n^A - \Psi_n^C) \rangle}{\langle \cos n(\Psi_n^B - \Psi_n^C) \rangle}}$$

Res{Ψ_n^A} is shown in the upper figure



Data-driven flow MC simulation

Reconstruct flow distribution by Monte Carlo simulation

Input parameter : v_2, v_3, v_4, χ_{42} , and $\text{Res}\{\Psi_2\}$

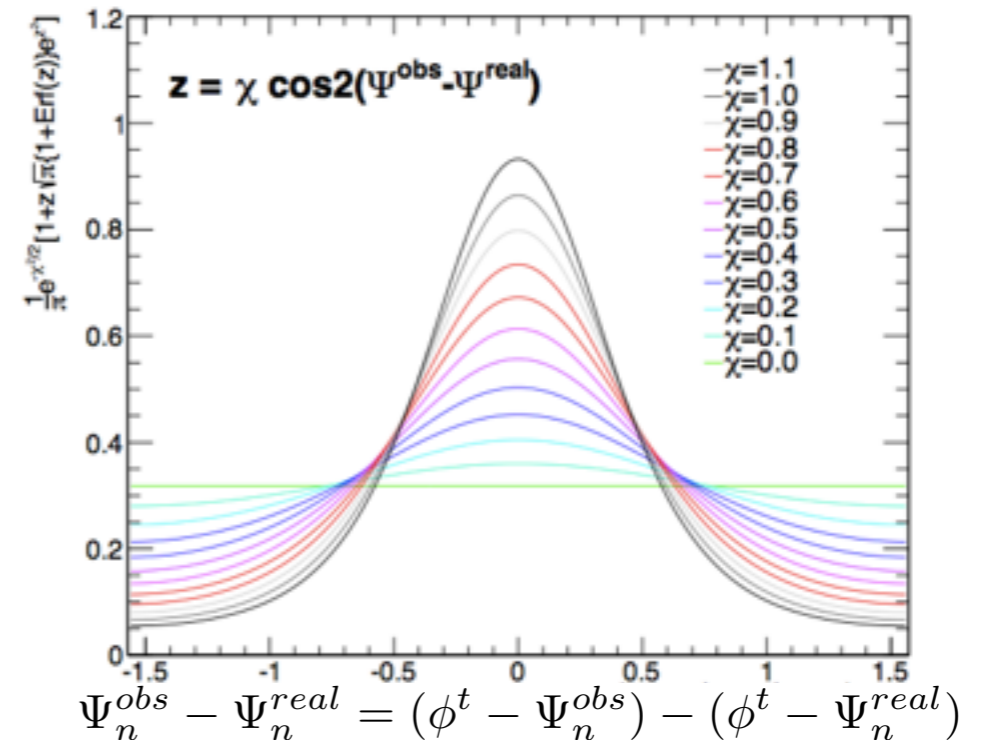
1. generate Ψ_2, Ψ_3 at random and Ψ_4 with considering correlation between Ψ_2 and Ψ_4
2. make flow distribution which reproduce v_n
3. smear trigger particle's angle with probability distribution when selecting trigger particles angle
4. generate particles at random along the flow distribution and calculate $\Delta\phi$

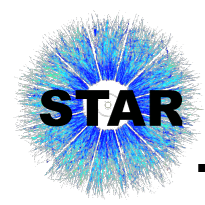
Probability distribution can be written with χ_n which is calculated with following formula :

$$\langle \cos[kn(\Psi_n^{obs} - \Psi_n^{real})] \rangle = \frac{\sqrt{\pi}}{2\sqrt{2}} \chi_n e^{-\chi_n^2/4} \left[I_{(k-1)/2} \left(\frac{\chi_n^2}{4} \right) + I_{(k+1)/2} \left(\frac{\chi_n^2}{4} \right) \right]$$

Jean-Yves OLLITRAULT, PRD 48 (1993) 1132

example of probability distributions of $\Delta\Psi_2$





Trigger smearing correction via fitting method

Assuming the associate-particles yield are distributed with respect to the event plane, we can correct the effect of trigger smearing due to the limited event-plane resolution which is **similar to the resolution correction in the flow measurement of the single particles.**

$$\frac{dN^{1+PTY}}{d(\phi^a - \Psi_2)} = 1 + Y(\phi_s, \Delta\phi)$$

$$= 1 + 2v_2^Y \cos 2(\phi_s + \Delta\phi) + 2v_4^Y \cos 4(\phi_s + \Delta\phi) \quad \dots(1)$$

$$\begin{aligned} \phi_s + \Delta\phi &= (\phi^t - \Psi_2) + (\phi^a - \phi^t) \\ &= \phi^a - \Psi_2 \end{aligned}$$

Applying a Fourier fitting eq.(3) to $1+Y(\phi_s, \Delta\phi)$ as a function of ϕ_s with a phase shift $\Delta\phi$, v_n^Y can be determined and the azimuthal distributions can be corrected with corrected v_n^Y by the event-plane resolution eq.(5).

$$\frac{dN_{cor}^{1+PTY}}{d(\phi^a - \Psi_2)} = 1 + 2\frac{v_2^Y}{\sigma_2} \cos 2(\phi_s + \Delta\phi) + 2\frac{v_4^Y}{\sigma_{42}} \cos 4(\phi_s + \Delta\phi) \quad \dots(2)$$

$$F(\phi_s)^{raw} = 1 + 2v_2^{raw} \cos 2(\phi_s + \Delta\phi) + 2v_4^{raw} \cos 4(\phi_s + \Delta\phi) \quad \dots(3)$$

$$F(\phi_s)^{cor} = 1 + 2\frac{v_2^{raw}}{\sigma_2} \cos 2(\phi_s + \Delta\phi) + 2\frac{v_4^{raw}}{\sigma_{42}} \cos 4(\phi_s + \Delta\phi) \quad \dots(4)$$

$$1 + Y^{cor}(\phi_s, \Delta\phi) = \frac{F(\phi_s)^{cor}}{F(\phi_s)^{raw}} \cdot (1 + Y^{raw}(\phi_s, \Delta\phi)) \quad \dots(5)$$

$$\begin{aligned} \sigma_2 &= \langle \cos 2(\Psi_2^{obs} - \Psi_2^{real}) \rangle \\ \sigma_{42} &= \langle \cos 4(\Psi_2^{obs} - \Psi_2^{real}) \rangle \end{aligned}$$



Trigger smearing correction via iteration method

bin-by-bin iterative unfolding correction method for $Y(\Delta\phi, \phi_s)$

Y^{raw} : yield before correction
 O : offset
 $A^{(n)}$: n-th corrected data
 $B^{(n)}$: n-th smeared correlation
 $C^{(n)}$: n-th correction function
 x, y : index of $\Delta\phi$ and ϕ_s
 Y^{corr} : yield after correction

input
(raw data) + offset

$$A^{(0)} = Y^{\text{raw}} + O$$



smeared (n-1)-th corrected data
for ϕ_s direction
with using probability distribution (P.21)

$$B^{(n)} = S A^{(n-1)}$$



make correction function
((n-1)-th corrected data) / (n-th smeared data)

$$C^{(n)}(x, y) = A^{(n-1)}(x, y) / B^{(n)}(x, y)$$



iteration

correction of raw data
with n-th correction function

$$A^{(n)}(x, y) = C^{(n)}(x, y) * A^{(0)}(x, y)$$



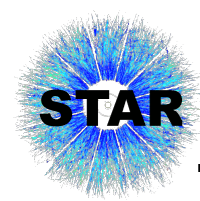
smooth correction function
with neighboring bins
with using smoothing parameter

$$C^{(n)}(x, y) = p_{\Delta\phi} \{C^{(n)}(x-1, y) + C^{(n)}(x+1, y)\} + p_{\phi_s} \{C^{(n)}(x, y-1) + C^{(n)}(x, y+1)\}$$

after converge

output
(corrected data) - offset

$$Y^{\text{corr}} = A^{(n)} - O$$



Sources of systematics

- ◆ v_2 , v_3 and v_4
 - including track cut, EP selection, and difference between $v_n\{\text{EP}\}$ and $v_n\{\text{2PC}\}$

- ◆ EP resolution
 - difference between East and West for trigger smearing in toy-MC

- ◆ EP correlation between different order harmonics
 - only Ψ_2 - Ψ_4 correlations

- ◆ $\Delta\phi$ range used for determination of zero-yield baseline
 - $\pi/6$ (default), $\pi/12$, $\pi/4$

- ◆ Trigger smearing correction
 - range of fitting method and iteration method
 - RMS of various smoothing parameter for ϕ_s and $\Delta\phi$